AFRRI TR86-3

AFRRI TECHNICAL REPORT

Ionization chamber intercomparison in mixed neutron and gamma-ray radiation fields by National Bureau of Standards and Armed Forces Radiobiology Research Institute

M. Dooley

L. J. Goodman

G. H. Zeman

R. B. Schwartz

C. M. Eisenhauer

P. K. Blake

DEFENSE NUCLEAR AGENCY

ARMED FORCES RADIOBIOLOGY RESEARCH INSTITUTE

BETHESDA, MARYLAND 20814-5145

REVIEWED AND APPROVED

Gary H. Zeman

GARY H. ZEMAN
CDR, MSC, USN
Chairman
Radiation Sciences Department

Lawrence S. Myers, Jr.

LAWRENCE S. MYERS, Ph.D.
Scientific Director

Richard I. Walker

RICHARD I. WALKER
CDR, MSC, USN
Acting Director

UNCLASSIFIED

SECURITY CLASSIFICATION OF THIS PAGE

REPORT DOCUMENTATION PAGE

1a. REPORT SECURITY CLASSIFICATION UNCLASSIFIED	1b. RESTRICTIVE MARKINGS
2a. SECURITY CLASSIFICATION AUTHORITY	3. DISTRIBUTION/AVAILABILITY OF REPORT Approved for public release; distribution unlimited.
2b. DECLASSIFICATION/DOWNGRADING SCHEDULE	
4. PERFORMING ORGANIZATION REPORT NUMBER(S) AFRRI TR86-3	5. MONITORING ORGANIZATION REPORT NUMBER(S)
6a. NAME OF PERFORMING ORGANIZATION Armed Forces Radiobiology Research Institute 6b. OFFICE SYMBOL (If applicable) AFRRI	7a. NAME OF MONITORING ORGANIZATION
6c. ADDRESS (City, State and ZIP Code) Defense Nuclear Agency Bethesda, Maryland 20814-5145	7b. ADDRESS (City, State and ZIP Code)
8a. NAME OF FUNDING/SPONSORING ORGANIZATION Defense Nuclear Agency 8b. OFFICE SYMBOL (If applicable) DNA	9. PROCUREMENT INSTRUMENT IDENTIFICATION NUMBER
8c. ADDRESS (City, State and ZIP Code) Washington, DC 20305	10. SOURCE OF FUNDING NOS. PROGRAM ELEMENT NO.: NWED QAXM PROJECT NO.: TASK NO.: WORK UNIT NO.: MJ 00137
11. TITLE (Include Security Classification) (see cover)	

12. PERSONAL AUTHOR(S)
Dooley, M., Goodman, L. J., Zeman, G. H., Schwartz, R. B., Eisenhauer, C. M., and Blake, P. K.

13a. TYPE OF REPORT	13b. TIME COVERED	14. DATE OF REPORT (Yr., Mo., Day)	15. PAGE COUNT
Technical	FROM ______ TO ______	December 1986	48

16. SUPPLEMENTARY NOTATION

17. COSATI CODES			18. SUBJECT TERMS (Continue on reverse if necessary and identify by block number)
FIELD	GROUP	SUB. GR.	

19. ABSTRACT (Continue on reverse if necessary and identify by block number)

This report describes a dosimetry intercomparison conducted between the Armed Forces Radiobiology Research Institute (AFRRI) and the National Bureau of Standards (NBS). The project was undertaken as part of an overall program to validate the reliability and credibility of the neutron dosimetry system used with the AFRRI TRIGA reactor in support of radiobiology research. The intercomparison included absorbed dose measurements with ionization chambers by the AFRRI Radiological Physics Division and the NBS Nuclear Radiation Division. Measurements were made at the NBS californium-252 facility using unmoderated and heavy-water-moderated configurations. At the AFRRI TRIGA reactor, measurements were done in four radiation fields, including unshielded, lead-shielded, and water-shielded configurations. All data were collected during the period July 1983 to March 1984. The agreement between results obtained by the two groups was good in the NBS californium-252 fields and excellent in the AFRRI reactor fields. Through the course of the study, the calibration procedures used at AFRRI were validated, and valuable data were collected on ionization chamber characteristics and the spatial variation of tissue kerma rates in the AFRRI

20. DISTRIBUTION/AVAILABILITY OF ABSTRACT UNCLASSIFIED/UNLIMITED ☒ SAME AS RPT. ☐ DTIC USERS ☐	21. ABSTRACT SECURITY CLASSIFICATION UNCLASSIFIED
22a. NAME OF RESPONSIBLE INDIVIDUAL Junith A. Van Deusen	22b. TELEPHONE NUMBER (Include Area Code) (202)295-3536 22c. OFFICE SYMBOL ISDP

DD FORM 1473, 83 APR EDITION OF 1 JAN 73 IS OBSOLETE.

UNCLASSIFIED

SECURITY CLASSIFICATION OF THIS PAGE

19. reactor exposure room. This report includes descriptions of the radiation sources, dosimetry methods, dosimetry results, and special dosimetry problems encountered during the work.

CONTENTS

INTRODUCTION

In 1983, the Radiological Physics Division at the Armed Forces Radiobiology Research Institute (AFRRI) embarked on an ambitious program aimed at upgrading the radiobiology dosimetry support at AFRRI. A key element in this upgrade was the evaluation of absorbed-dose measurements with ionization chambers in the mixed neutron and gamma-ray fields of the AFRRI TRIGA (Training Research Isotopes General Atomics) reactor. As part of the evaluation, an intercomparison of neutron dosimetry was carried out with the Nuclear Radiation Division of the National Bureau of Standards (NBS).

Before this effort, AFRRI had last compared its neutron ionization chamber measurements with other laboratories in 1973, when it participated in the International Neutron Dosimetry Intercomparison sponsored by the International Commission on Radiation Units and Measurements (1). Since that time, an increased interest in neutron radiotherapy has instigated the collection of considerable data on the basic physical parameters used for neutron dosimetry (2-6). Further, recent completion of the neutron spectral characterization of several AFRRI reactor fields (7,8) has enabled the calculation of the tissue-kerma factors needed for ionization chamber measurements in these fields (9). In conjunction with these efforts to improve the data base, protocols were established to standardize the methodology and terminology used in neutron dosimetry (10-12).

The availability of these physical data and the implementation of documented procedures made it essential for AFRRI to validate its mixed-field dosimetry techniques and to provide a foundation for future dosimetry programs between AFRRI and NBS. The intercomparison included measurements with ionization chambers in the NBS californium-252 facility and in four frequently used radiation fields of the AFRRI reactor. Scientists at AFRRI and NBS determined the tissue-kerma and absorbed-dose rates from the measurements and then compared results. In addition, the AFRRI chamber calibration procedures were examined through a comparison of chambers calibrated at the NBS and the AFRRI cobalt-60 facilities. This report summarizes the intercomparison, including a brief description of the sources, methods, results, special dosimetry problems, and accomplishments of the project.

MATERIALS AND METHODS

The intercomparison was accomplished through four sessions of measurement, with 2 weeks at the NBS radiation facilities and 2 weeks at the AFRRI reactor (see Appendix A).

The first set of measurements was performed in July 1983 at the NBS californium-252 irradiation facility, to take advantage of the well-known fission neutron spectrum and emission rate from the californium source (13,14). Free-in-air tissue-kerma rates were calculated from data that had been collected with ionization chambers exposed to an unmoderated californium-252 source and the same source moderated with a sphere of heavy water (D_2O). A second set of measurements was performed in November 1983 to resolve some ambiguous data

and discrepancies between AFRRI and NBS results. At that time, the calibration procedures of AFRRI were checked by calibrating four AFRRI chambers at the NBS cobalt-60 calibration facility.

Measurements were also performed in four configurations of the AFRRI reactor. Preliminary measurements were made in July 1983, followed by a definitive set of measurements completed in March 1984.

The Materials and Methods section provides a brief description of the sources, the instrumentation, and the measurement and calibration techniques used in the intercomparison.

RADIATION FACILITIES

NBS Californium-252 Facility

The NBS californium source used in this study is designated NS-100, and it was approximately 0.84 mg in July 1983. The source, fabricated for NBS by the Oak Ridge National Laboratories, is lightly encapsulated in about 3.2 mm of aluminum and 2.2 mm of stainless steel. With the moderator in place, the source was surrounded by a sphere of D_2O (radius 15.3 cm) covered with a thin sheet of cadmium (0.8 mm). The source was raised and lowered manually with a string from a shielded portion of the exposure facility. Each chamber was exposed individually in free air, at a nominal distance of 30 cm from the center of the source. When raised into position, the source was about 2.7 m from the concrete floor and 4 m from the nearest wall, making the contribution of room-backscattered neutrons negligible, i.e., less than a calculated value of 0.5% of the tissue-equivalent (TE) chamber response (14). Figure 1 diagrams the arrangement.

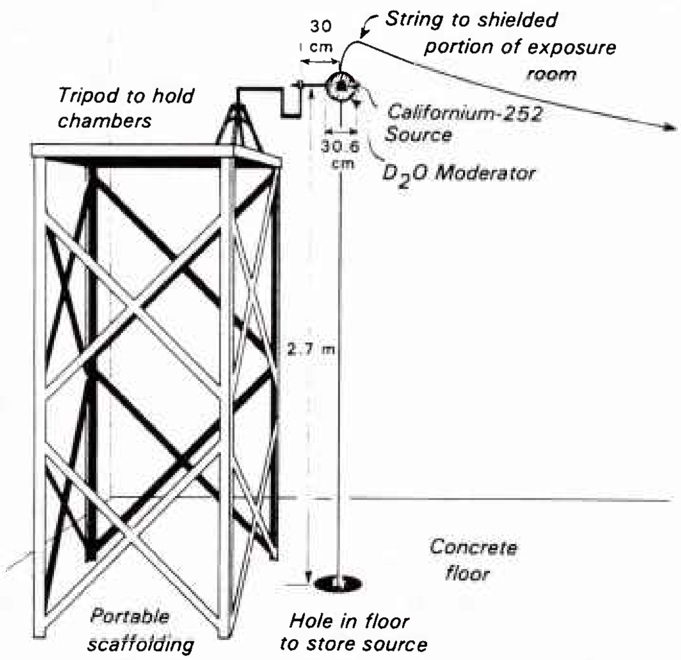

Figure 1. Arrangement of californium irradiation facility

AFRRI TRIGA Reactor

The AFRRI TRIGA reactor is described in reference 15. All measurements were performed in exposure room 1 (ER1) of the reactor facility. ER1 is approximately 6.1 m by 6.1 m by 2.6 m high, with a semicylindrical lobe of the reactor tank protruding into the south wall. The tank wall is covered with cadmium, and the exposure room surfaces (walls, floors, and ceiling) are coated with gadolinium paint to absorb thermal neutrons.

Measurements were conducted in four of the most frequently used reactor configurations (Table 1 and Figure 2), described in the following:

15-cm-Pb shield: A 15-cm-thick lead shield placed in front of the reactor tank wall to attenuate fission and fission product gamma radiation

Bare room: No shielding placed between the experiment and the reactor core

30-cm-water shield: Reactor core moved back 30 cm from its nominal position in the tank, creating a water shield to drastically reduce the neutron component of the radiation field

15-cm-Pb field with phantom: A 15-cm-diameter, 24-cm-high cylindrical phantom placed behind the lead shield (configuration 1). The phantom, shown in Figure 3, was constructed of plastic and filled with TE liquid (liquid number 33 in Appendix B of reference 10).

Table 1. Reactor Configurations

Number	Configuration	Meters From Core Center*
1	15 cm Pb	100, 235, 328, 401
2	Bare room	100, 235, 328, 401
3	30 cm water	130
4	15 cm Pb with phantom	100

*Nominal distance from front face of tank wall to core center was 30 cm.

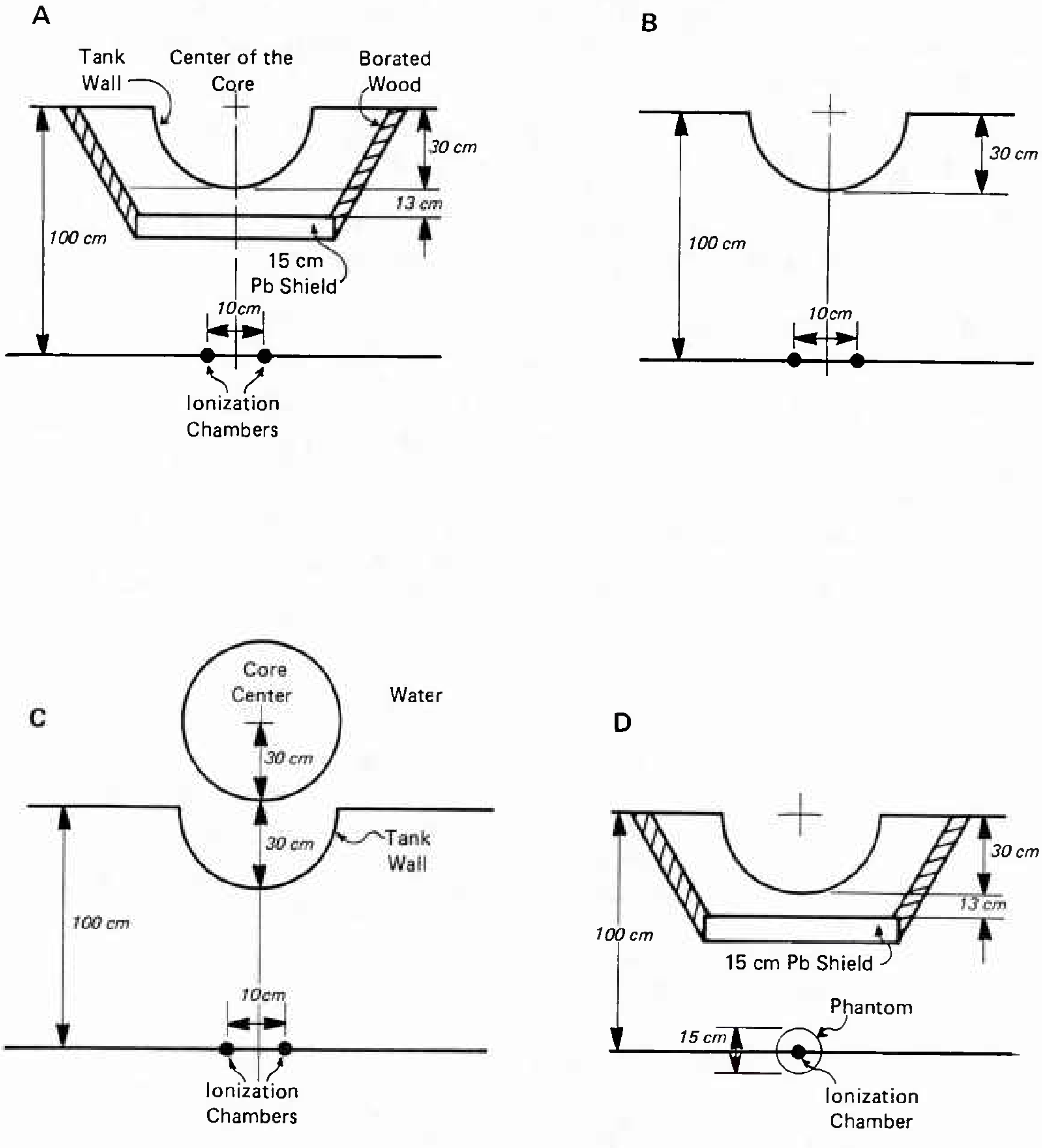

Figure 2. Reactor configurations: A, configuration 1; B, configuration 2; C, configuration 3; D, configuration 4.

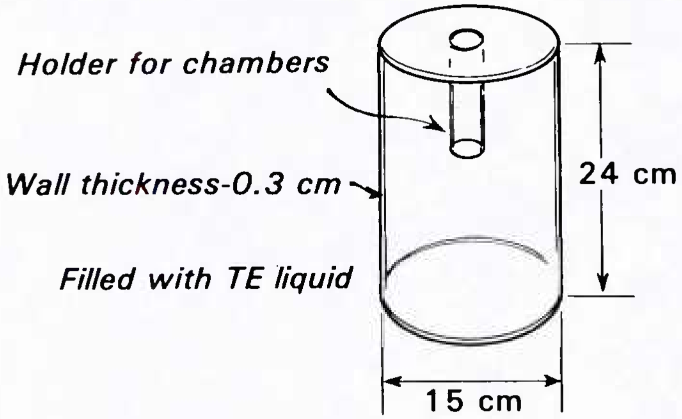

Figure 3. Plastic phantom used in intercomparison

In all configurations, measurements were made with the chambers 120 cm above the floor and 70 cm from the tank wall. This is a nominal distance of 100 cm from the reactor core center in configurations 1, 2, and 4, and 130 cm from the center of the core in configuration 3. To investigate the spatial variation within the exposure room, measurements were also performed in the lead-shielded and bare configurations at three additional distances ranging from 1 to 4 m from the core. AFRRI and NBS chambers were irradiated simultaneously, spaced about 10 cm apart and equidistant from the core centerline (see Figure 4) in all configurations except inside the phantom, where they were exposed individually. The neutron and gamma-ray spectra in each of these configurations are given in reference 7.

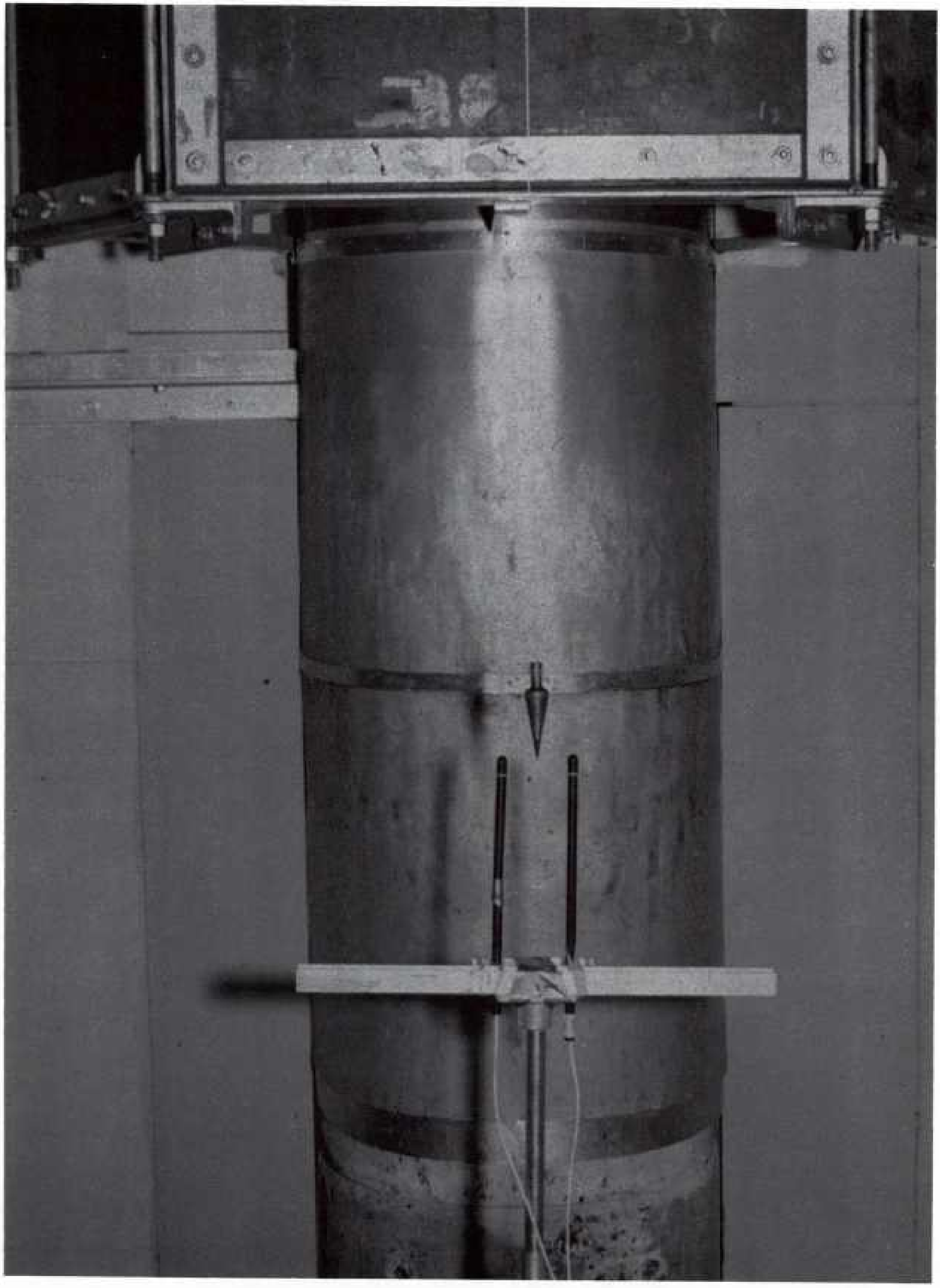

Figure 4. Two chambers set up in ER1 with no shield. (Note the plumb bob used for chamber positioning.)

DOSIMETRY SYSTEMS

The two-dosimeter method described in reference 10 was used to measure the neutron and gamma-ray tissue-kerma rates in free air and the absorbed-dose rate at the midline of a phantom. The NBS and AFRRI groups each used a pair of 0.5-cm^3 Exradin (Warrenville, IL) ionization chambers consisting of an A150 plastic TE chamber (Model T2) filled with methane-based TE gas (TE/TE chamber) and a magnesium chamber (Model MG2) with argon gas (Mg/Ar chamber). The gas flow rate through the chambers was approximately 30 cm^3/min. The composition of A150 plastic and TE gas are given in Appendix B of reference 10. In addition to the Mg/Ar chamber, the NBS dosimetrists substituted a Geiger Mueller (GM) proportional counter as the nonhydrogenous instrument of the dosimeter pair. The GM chamber was used in both configurations of the californium-252 facility, but was used only in the lead-shielded configuration of the reactor because the high background radiation from the core was too high for this sensitive dosimeter. The AFRRI group also used a second set of chambers in the californium-252 facility, consisting of two 50-cm^3 spherical chambers constructed at AFRRI (16). An A150 plastic chamber with TE gas provided the TE/TE portion of the pair, and a graphite chamber with carbon dioxide gas (Gr/C) served as the nonhydrogenous instrument. Both chambers used a gas flow rate of about 80 cm^3/min. Due to time constraints, the 50-cm^3 chambers were not used in the AFRRI reactor irradiations.

The NBS chambers were connected (via signal cables) to a Keithley Instruments, Inc. (Cleveland, OH) 642 electrometer through the accompanying remote preamplifier. The electrometer signal was fed to a scaler controlled by a timer. The collected counts per time interval were manually entered into a Hewlett-Packard (HP) (Corvallis, OR) 85 desktop computer, which calculated the charge per unit time. A collecting potential of + or - 400 volts was applied across the chamber through an Ortec, Incorporated (Oak Ridge, TN) high-voltage source.

The AFRRI chambers were connected to a Keithley 616 electrometer with the collecting potential (+ or - 400 volts for the 0.5-cm^3 chambers and + or - 1000 volts for the 50-cm^3 chambers) supplied by an Ortec high-voltage source. The system was semiautomated in that the electrometer signal was sampled at set time intervals by an HP 3421A data acquisition unit, which was controlled by an HP 85 desktop computer. The electrometer readings were stored by the computer and used to calculate the charge accumulated per time interval. Figure 5 is a photograph of the AFRRI data acquisition system.

CALIBRATIONS

Dosimetry using ionization chambers is generally based on the calibration of the ionization chambers in cobalt-60 or cesium-137 gamma-ray beams. The chambers used by the NBS group were calibrated using the standard cobalt-60 gamma-ray machine at NBS. AFRRI chambers were calibrated using the Theratron-80 cobalt-60 machine at AFRRI (17), which had been calibrated with an AFRRI ionization chamber calibrated in the standard NBS cobalt-60 beam. To verify that the traceability to the NBS standard had been properly transferred to AFRRI, four

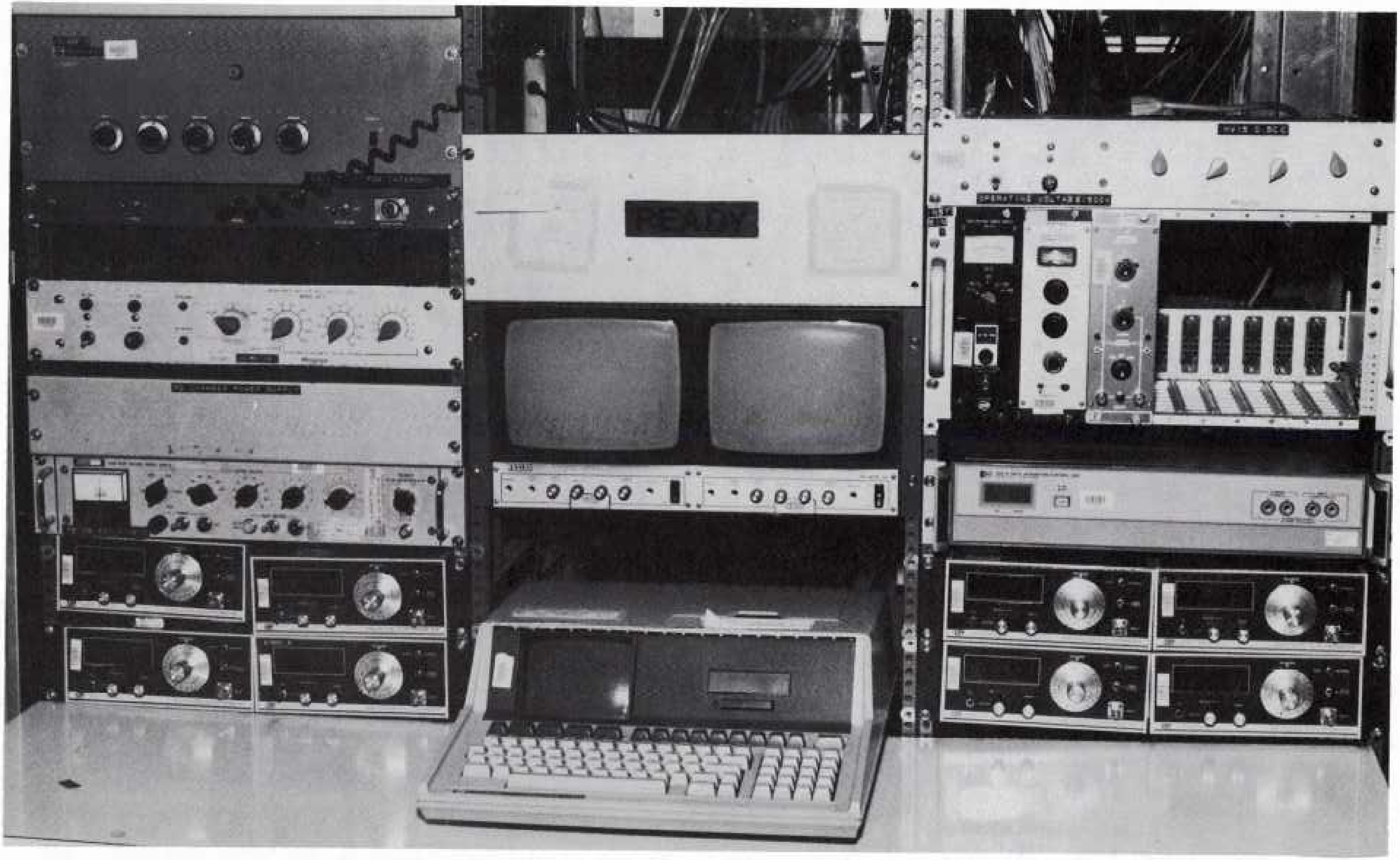

Figure 5. AFRRI data acquisition system

AFRRI chambers were calibrated directly in the NBS cobalt-60 beam. The calibration factors obtained at NBS for each chamber, N_x in roentgens per coulomb (R/C), were compared to the calibrations performed at AFRRI.

The absorbed-dose calibration factor, α_c (Gy/C), was calculated from the exposure calibration factor:

$$\alpha_c = N_x f_c K_w$$

where f_c = 9.62×10^{-3} Gy/R (reference 18) and represents the exposure-to-tissue absorbed-dose conversion factor for cobalt-60 photons

K_w = wall attenuation and scatter correction factor for the cobalt-60 beam

The wall correction factor (K_w) is necessary when measuring the tissue kerma in free air to determine the effect of the chamber wall. This factor need not be evaluated for in-phantom measurements because the chamber wall can be considered as part of the phantom if the composition of the chamber is similar to that of the phantom. In free air, the chamber wall both attenuates the incident radiation and scatters radiation into the sensitive volume of the chamber. Attenuation usually dominates over scatter; therefore, the response of the chamber decreases as the wall thickness increases past the thickness required for secondary particle equilibrium. To evaluate K_w, measurements were made with buildup caps of various thicknesses placed on the chamber. The chamber response with zero wall thickness was found by extrapolating the graph of response versus wall thickness to zero wall thickness. K_w was then computed as the ratio of the chamber response at the operating wall thickness to the theoretical response at zero wall thickness.

MEASUREMENTS

Paired-Chamber Equations

The measurement principles and techniques used throughout the intercomparison are described in reference 19. The neutron and gamma-ray kerma and absorbed-dose rates were calculated from the measured chamber responses using the following equations:

$$R_t' = k_t D_n + h_t D_g$$

$$R_u' = k_u D_n + h_u D_g$$

In these equations, known as the paired-chamber equations, the subscript t refers to the TE/TE chamber and u refers to the nonhydrogenous (Mg/Ar, GM, or Gr/C) chamber. The terms are defined as follows:

R_t', R_u' = Chamber response in the mixed field relative to its response to gamma rays used for calibration, cobalt-60 in this case (units: Gy [cobalt-60])

k_t, k_u = Response of each chamber to neutrons in the mixed field relative to its response to calibration gamma rays (units: Gy [cobalt-60]/Gy [mixed field])

h_t, h_u = Response of each chamber to gamma rays in the mixed field compared to the calibration gamma rays (units: Gy [cobalt-60]/Gy [mixed field])

D_n, D_g = Neutron and gamma-ray tissue kerma in free air or tissue-absorbed dose in Gy

By rearranging the above equations, the separate neutron and gamma-ray kerma or absorbed doses are given explicitly by:

$$D_n = \frac{h_u}{(h_u k_t - h_t k_u)} R_t' + \frac{-h_t}{(h_u k_t - h_t k_u)} R_u'$$

$$D_g = \frac{-k_u}{(h_u k_t - h_t k_u)} R_t' + \frac{k_t}{(h_u k_t - h_t k_u)} R_u'$$

The relative chamber responses (k_t, k_u, h_t, h_u) are spectrum dependent, and are discussed in detail in reference 19. The relevant physical parameters for each configuration are provided in Table 2, and the calculation of k_t is shown in Appendix B. Because the values of h_t and h_u are close to unity, the assumption $h_t = h_u = 1$ was made for all configurations.

Table 2. Values of Physical Parameters

Parameter	Californium-252	Californium-252 Moderated	15 cm Pb	Bare Room	30 cm Water
E_n (MeV)	2.7	2.6	1.7	2.6	4.8
W_n, MTE gas (eV)	31.6	32.5	32.2	32.0	31.7
W_n/W_c (W_c = 29.3 eV)	1.078	1.109	1.099	1.092	1.082
K ICRU* muscle (1E-11 Gy cm^2)	2.9	0.79	1.52	1.96	2.76
K A150 plastic (1E-11 Gy cm^2)	2.98	0.812	1.54	2.02	2.83
K MTE gas (1E-11 Gy cm^2)	2.95	0.803	1.54	2.00	2.80
k_t, TE/TE (0.5 cm^3)	0.948	0.922	0.922	0.939	0.943
k_t, TE/TE (50 cm^3)	0.944	0.917	0.922	0.934	0.938
k_u, Mg/Ar	0.033	0.005	0.01	0.02	0.025
k_u, GM	0.003	0.003	0.002	0.002	0.003
k_u, Gr/C	0.06	0.005	0.02	0.03	0.055
h_t, TE/TE	1.0	1.0	1.0	1.0	1.0
h_u, Mg/Ar, GM, Gr/C	1.0	1.0	1.0	1.0	1.0

*International Commission on Radiation Units and Measurements

Chamber Response

The relative chamber responses, R_t' and R_u', were computed from the chamber reading R, in coulombs (C), using:

$$R' = R \cdot \alpha_c \cdot K_{tp} \cdot K_s/K_w$$

where α_c (Gy/C) = the cobalt-60 tissue-absorbed dose calibration factor

K_{tp} = corrects ambient temperature and pressure to standard temperature and pressure:

$$K_{tp} = \frac{(T + 273.15)}{295.15} \times \frac{760}{P}$$

where T is temperature in Celsius and P is atmospheric pressure in mm of mercury

K_s = ion recombination (saturation) correction

K_w = chamber wall attenuation and scatter correction

The chamber reading R was measured by integrating the ionization charge for a set time interval (between 10 and 30 sec) while the source was in place and, in the case of the reactor, at power. The system noise, or drift, was measured both before and after the chamber was irradiated, and the mean of the pre- and postirradiation drifts was used to compensate the reading to determine the net charge accumulated during irradiation. That is,

$$R = R_c - R_d$$

where R = chamber reading compensated for drift

R_c = average charge collected with source on

R_d = average of pre- and postirradiation drifts

In the californium-252 facility, the drift charge was integrated with the source in its storage position. At the reactor, the drift was measured with the core in place but not at power, and it therefore included residual radiation from the power runs. Although at least some of the residual radiation is part of the measured gamma component of dose or kerma, it was subtracted to maintain consistency in the measurements. Several measurements of the drift and the ionization current were performed, using both positive and negative collecting potentials across the chamber. Measurements at the californium-252 facility were normalized to time, and all measurements in ER1 were normalized to the response of a 50-cm^3 air-filled TE monitor chamber fixed to the ceiling of the exposure room (shown in Figure 6).

The ion recombination correction was determined by measuring the chamber response at several values of collecting potential. For neutrons, initial (intratrack) recombination is usually dominant over general (intertrack) recombination, and the chamber response at an infinite collecting voltage is found by extrapolating the plot of 1/R against 1/V to 1/V = 0. At high dose rates, general recombination usually dominates, and then the plot of 1/R versus $1/V^2$ is extrapolated to $1/V^2 = 0$ (reference 20). Because the dose rates were very low in these measurements, the 1/V method was appropriate.

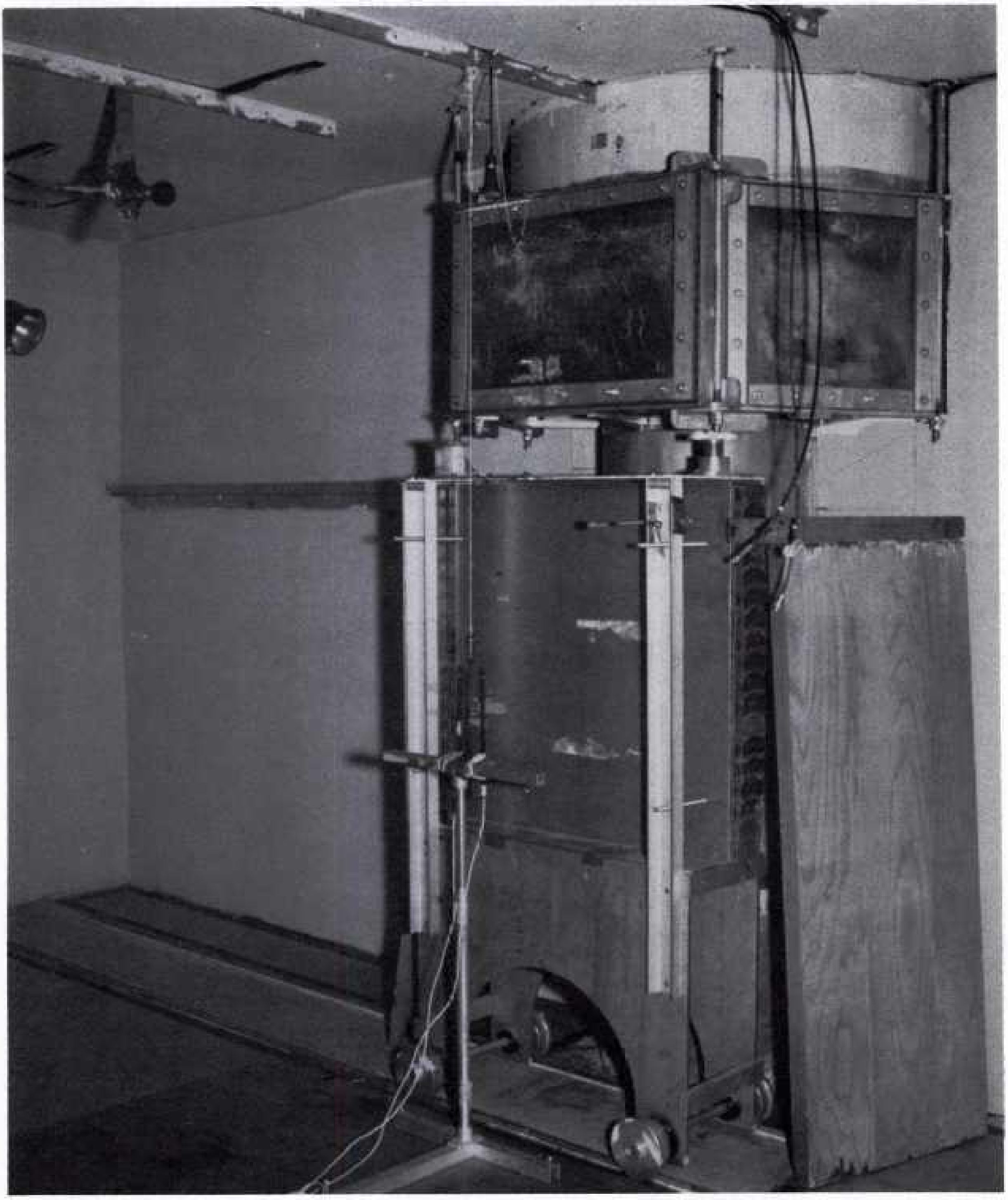

Figure 6. Ion chambers set up in ER1 with 15-cm-Pb shield. (Note the spherical monitor chamber mounted in the ceiling.)

The wall correction factors, K_W (discussed in section on Calibrations), were evaluated in the moderated californium-252 exposure field and in configurations 1, 2, and 3 of the AFRRI TRIGA reactor. Wall correction data were available from previous measurements for the 0.5-cm^3 Exradin chambers in the unmoderated californium-252 field (21), and these measurements were not repeated.

RESULTS

CHAMBER CORRECTION FACTORS

The chamber correction factors evaluated for this study are shown in Table 3. Note that all data were used except the wall data collected with the 0.5-cm^3 chambers using the moderated californium-252 source, which were inconclusive. As a result of these poor data, the kerma calculated from the 0.5-cm^3 chamber data could not be separated into the neutron and gamma-ray components.

Table 3. Chamber Correction Factors

Chamber	Factor	Co-60	Cf-252 Unmod	Cf-252 Mod	Reactor 15-cm Pb	Reactor Bare	Reactor 30-cm H_2O
TE/TE (0.5 cm^3)	K_W*	0.992 (2mm cap)	0.969	0.984	0.984	0.976 (3mm cap)	0.995 (5mm cap)
	K_S	1.00	1.002	1.002	1.002	1.002	1.000
Mg/Ar (0.5 cm^3)	K_W	0.989 (1mm cap)	0.961	0.725	0.988	0.986 (2mm cap)	0.995 (5mm cap)
	K_S	1.00	1.006	1.006	1.006	1.006	1.00
TE/TE (50 cm^3)	K_W	0.978	0.921	0.970	—	—	—
	K_S	1.00	1.00	1.00	—	—	—
Gr/C (50 cm^3)	K_W	0.979	0.959	0.973	—	—	—
	K_S	1.00	1.00	1.00	—	—	—

*Wall thicknesses of 0.5-cm^3 and 50-cm^3 chambers without buildup caps are approximately 1 and 7 mm, respectively.

COBALT-60 CALIBRATIONS

The results of the cobalt-60 calibration of the four AFRRI ionization chambers are shown in Table 4. The ratio of the calibration factors (AFRRI/NBS) determined at the two different cobalt-60 facilities varies from unity by 2% or less for three of

the four chambers, which is good precision for this comparison. However, for the 50-cm^3 chamber TE10, a difference of 5% in the calibration factors was obtained. The value in parentheses indicates that when the chamber was recalibrated at AFRRI, it differed with the NBS calibration by only 0.8%. Thus, the direct cobalt-60 calibration of AFRRI chambers with the NBS standard beam served not only to verify the correct calibration of the AFRRI machine but also to discover an inaccurately calibrated chamber.

Table 4. Calibration Results

Chamber	Exposure Calibration Factor (R/nC)	AFRRI/ NBS	K_w
TE 118 (0.5 cm^3)	5.473	0.993	0.992 (2-mm cap)
Mg 111 (0.5 cm^3)	3.740	1.019	0.989 (1-mm cap)
TE 10 (50 cm^3)	0.06114	1.054 (0.992)*	0.978 (no cap)
Grl A (50 cm^3)	0.04474	1.016	0.979 (no cap)

*Result of recalibration at AFRRI

CALIFORNIUM-252

Tissue-kerma rates measured by NBS and AFRRI at the NBS californium-252 facility are shown in Table 5. The measured total (neutron plus gamma ray) kerma rate, K_T, compared well in both the unmoderated and D_2O-moderated configurations. The measured neutron and gamma kerma rates (K_n and K_g) in the unmoderated field did not agree as well, with the largest discrepancies seen in the 50-cm^3 chamber results. However, in the moderated field, the 50-cm^3 chambers agreed very well with the NBS TE-GM dosimeter pair. Although the K_T measured with both the AFRRI and NBS TE-Mg dosimeter pairs agreed well with that measured with the 50-cm^3 chambers and the TE-GM pair, the two radiation components could not be resolved because of the extreme difficulty in measuring the low ionization current ($<10^{-14}$ A) produced in the small (0.5 cm^3) chambers.

The differences obtained in these measurements are reasonable, considering that the source intensity was insufficient to allow optimal precision of measurement. Table 5 implies that a precision of about 3% was achieved for the determination of the total kerma, and a precision of about 9% was achieved for the separate neutron and gamma-ray components.

Table 5. Californium-252 Results

Configuration	Dosimeter Pair	K_n (mGy/h)	K_g (mGy/h)	K_t (mGy/h)	K_g/K_t
Unmoderated	NBS TE-GM	19.2	9.6	28.8	0.33
	NBS TE-Mg	19.9	8.9	28.8	0.31
	AFRRI TE-Gr	18.5	10.4	28.9	0.36
	AFRRI TE-Gr*	20.2	9.8	30.0	0.33
	AFRRI TE-Mg	19.1	9.8	28.9	0.34
Moderated	NBS TE-GM	4.0	8.6	12.6	0.68
	NBS TE-Mg	—	—	12.4	—
	AFRRI TE-Gr	4.1	8.6	12.7	0.68
	AFRRI TE-Mg	—	—	12.7	—

*Second set of measurements

AFRRI TRIGA REACTOR

Table 6 gives the results of the measurements performed in ER1 of the AFRRI reactor. Although the chamber response was normalized to the response of the monitor chamber, the results are listed here in terms of integrated power (kilowatt · minute), a more meaningful term to most readers. The response of the monitor to reactor power is provided in Appendix C. Also in Appendix C are the relationships used to convert from µGy/pCm (microgray per picocoulomb monitor) to cGy/kW · min (centigray per kilowatt · minute). The precision of the chambers was better than 2% in almost all cases.

15-Cm-Pb Shield and 15-Cm-Pb Shield With Phantom

The effect of the 15-cm-Pb shield was to reduce the gamma-ray component of kerma to approximately 10% of the total. In this predominantly neutron field, the NBS- and AFRRI-measured neutron (K_n), gamma-ray (K_g), and total (K_T) kerma rates are in excellent agreement. The differences in K_T are all less than 1%, and the neutron and gamma-ray components differ by 3% or less. In the phantom, the measured neutron, gamma-ray, and total kerma rates of the two groups are within 1% of each other.

Table 6. Reactor Results

Reactor Configuration	Meters From Core Center	Group	cGy/kW · min			
			K_n	K_g	K_T	K_g/K_T
15 cm Pb	1.00	NBS*	7.14	0.700	7.84	0.09
		NBS†	7.14	0.714	7.85	0.09
		AFRRI	7.17	0.700	7.87	0.09
	2.35	NBS†	0.742	0.560	1.30	0.43
		AFRRI	0.750	0.553	1.30	0.42
	3.28	NBS†	0.334	0.433	0.767	0.56
		AFRRI	0.333	0.428	0.761	0.56
	4.01	NBS†	0.199	0.373	0.571	0.65
		AFRRI	0.202	0.365	0.567	0.64
In phantom	1.00	NBS†	2.21	1.210	3.420	0.35
		AFRRI	2.19	1.220	3.400	0.35
Bare Room	1.00	NBS*	12.2	24.9	37.1	0.67
		NBS†	12.5	24.6	37.1	0.66
		AFRRI	12.2	24.6	36.8	0.69
	2.35	NBS†	1.88	5.09	6.97	0.73
		AFRRI	1.91	5.02	6.93	0.72
	3.28	NBS†	1.02	2.98	4.00	0.74
		AFRRI	0.99	2.96	3.95	0.75
	4.01	NBS†	0.476	2.36	2.84	0.83
		AFRRI	0.628	2.21	2.84	0.78
30 cm Water	1.30	NBS†	—	4.69	4.69	1.00
		AFRRI	—	4.67	4.67	1.00

*NBS pair T2-M2

†NBS pair T2-MG131

Bare Room

The bare-room field consists mainly of gamma rays, with the contribution of the neutrons ranging from about 30% at 1 m to less than 2% at 4 m from the reactor core center. In this field, better than 1% agreement was again seen between the NBS- and AFRRI-measured total kerma rates. The gamma-ray kerma rates, which constituted most of the total, also agreed to within 1% of each other at distances up to 3 m from the core center, but a 6% difference was seen at the 4-m position. Similarly, the neutron kerma rates compared well close to the core (1%-4% up to 3 m), but the measured values at 4 m differed by 30%.

30-Cm-Water Shield

With the reactor core moved back 30 cm, the neutron kerma was almost completely attenuated, and the two components of the kerma could not be resolved using the paired-chamber method. However, the agreement for the measured total kerma rates was within 1%. The wall attenuation and scatter data indicate that the radiation produced in this configuration consists predominantly of fairly hard gamma rays, resulting in part from neutron capture by hydrogen in the water ($H[n,\gamma]^2H$). The TE and Mg chambers both required a wall thickness of 6 mm to attain electronic equilibrium. (For comparison, a wall thickness of only about 3 mm is sufficient to attain electronic equilibrium for cobalt-60 photons.)

Summary of Reactor Results

NBS and AFRRI tissue-kerma and absorbed-dose rate measurements compared very well in all the reactor fields. The best comparisons were in the configurations where most of the kerma resulted from neutrons (configurations 1 and 4). In the predominantly gamma-ray fields, the total kerma compared well at all distances. Although the neutron and gamma-ray components also compared well at the 1-m and 2-m positions, these comparisons grew progressively poorer at larger distances from the core.

DISCUSSION

The results reviewed above show good agreement between NBS and AFRRI tissue-kerma rates measured at the NBS californium-252 facility, and excellent agreement of the measured tissue-kerma and absorbed-dose rates in the different fields of the AFRRI reactor. In addition to demonstrating sound dosimetry techniques, the intercomparison allowed the collection of much needed data pertaining to ionization chamber characteristics as well as the spatial variations in two configurations in ER1. Discussed below are some of the implications of the data and relevant lessons learned through the data-collecting process.

MODERATED CALIFORNIUM-252 SOURCE

The measurements of the ionization current from the D_2O-moderated californium-252 source stretched the capabilities of the 0.5-cm^3 chambers. In both sets of measurements, the wall attenuation and scatter data were inconclusive, and the precision in the second set of measurements was as poor as 20% due to unexplained system noise and instabilities. Under these measurement conditions, ionization currents less than about 10^{-13} A (~2 R/h) cannot be measured precisely with the 0.5-cm^3 chambers.

MG CHAMBER OVERRESPONSE TO NEUTRONS

During the course of measurements in the 15-cm-lead shield configuration, the NBS Mg/Ar chamber (designated MG2) consistently responded about 25% higher than did the AFRRI Mg/Ar chamber. An investigation of this discrepancy (involving interchanges of chambers, gas supplies, electrometers, and cables) led to the conclusion that the NBS chamber was in fact overresponding to the neutrons in this field. The response of the suspect chamber to gamma rays appeared to be correct, which was verified by checking the chamber calibration with the AFRRI Theratron-80 cobalt-60 source. Although the response of MG2 did not appear to be affected in the bare configuration, it was decided not to use the defective chamber at all. The manufacturer later stated that the inner surface of the chamber was probably contaminated.

This incident served as a reminder that, to ensure the proper operation and stability of ion chambers, it is essential to have some means (e.g., a neutron check source) of assessing the neutron sensitivity of TE as well as Mg chambers. Without a method of checking the neutron response, a defective chamber, such as MG2, could go undetected indefinitely because its unchanged response to cobalt-60 may give a false sense of security.

SPATIAL VARIATIONS IN ER1

Data were collected in the bare room and behind the 15-cm-Pb shield to evaluate how the neutron and gamma-ray kerma rates vary with distance from the reactor core. These measurements were also compared with the response predicted by the calculations in reference 7. (The calculations were performed only for the bare-room configuration using a one-dimensional ANISN code.) In Figures 7-9, the measured and calculated kerma rates multiplied by the square of the distance to the center of the core (Kr^2) are plotted as a function of the distance squared (r^2) in the bare and Pb-shielded configurations. A horizontal line on these plots would indicate $1/r^2$ behavior.

In Figure 7, the plots of Kr^2 versus r^2 for photons are shown for the 15-cm-Pb-shielded and the bare configurations. In both configurations, the data increase approximately linearly with distance squared. Also, the bare-room data agree reasonably well with the calculations for a spherical configuration (7).

Figures 8 and 9 show the variation of Kr^2 versus r^2 for neutron kerma in the Pb-shielded and bare configurations, respectively. In the Pb-shielded configuration, the measured data indicate a decrease with distance from the core center. The measured neutron kerma rate at the 1-m position is about 20% lower than the calculated value. In the bare room, the calculated neutron kerma rate at 1 m agrees well with the measured neutron kerma rate. However, in contrast to the measurements, the calculations predict a slow increase in Kr^2 with distance squared and only a slight deviation (<10%) from $1/r^2$ at 1 m.

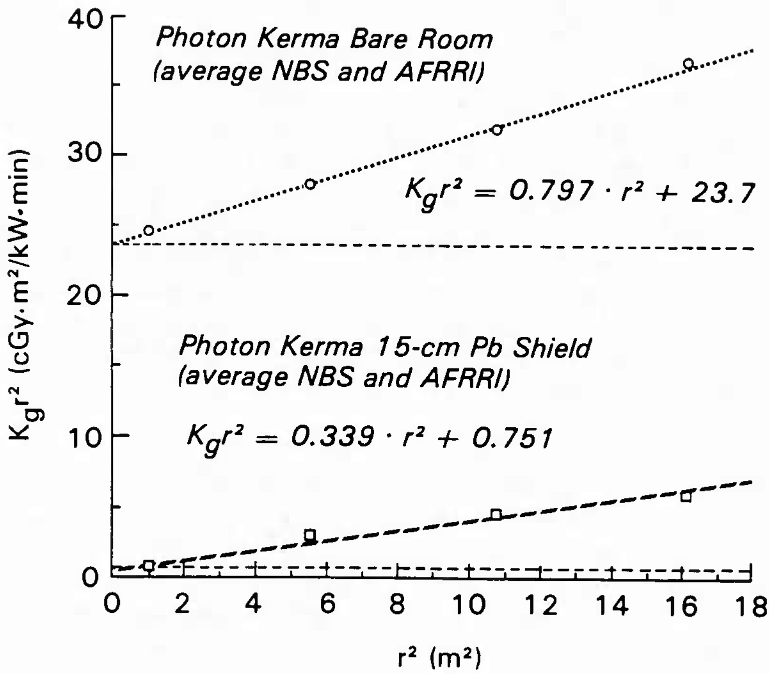

Figure 7. Photon $1/r^2$ measurements (with 15 cm Pb or bare room)

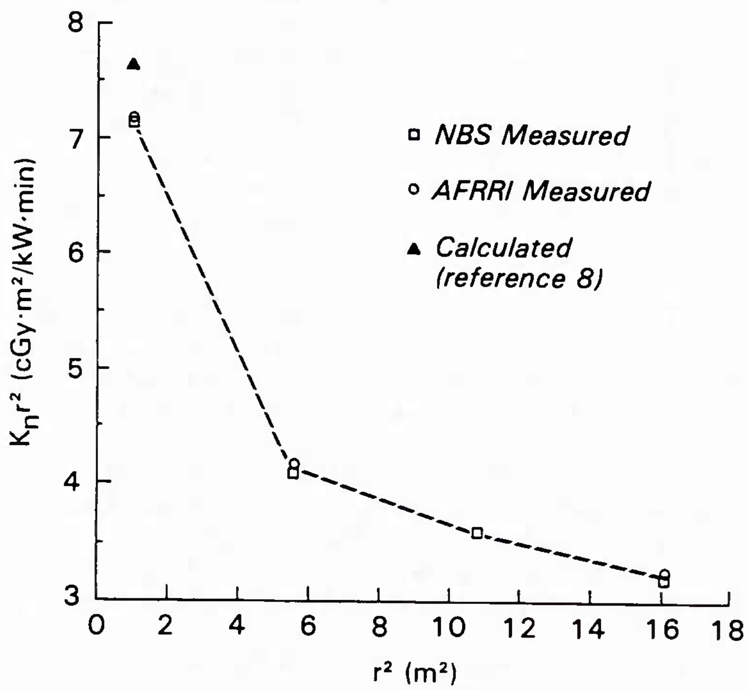

Figure 8. Neutron $1/r^2$ measurements with 15 cm Pb

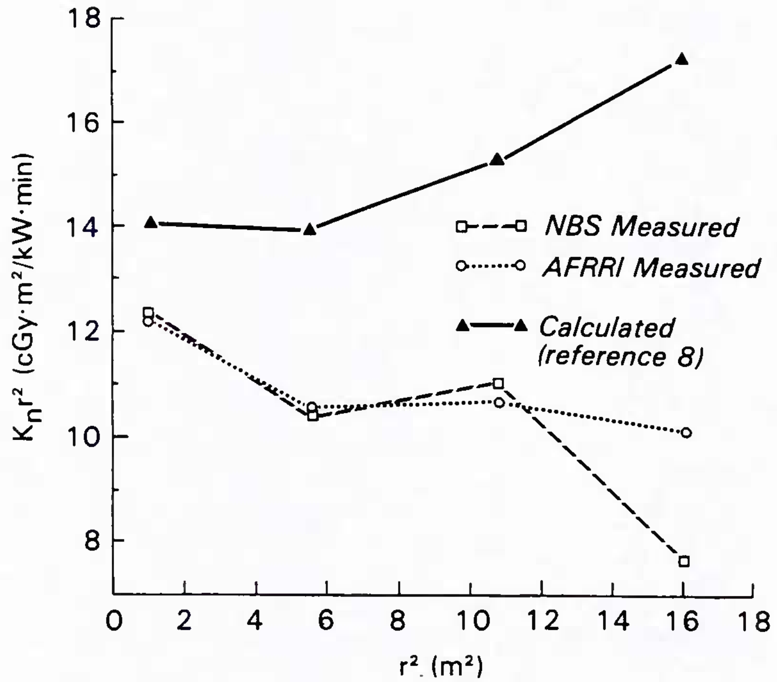

Figure 9. Neutron $1/r^2$ measurements with bare room

Clearly, the neutron kerma rates in the Pb-shielded and the bare configurations do not show $1/r^2$ behavior, if the reactor core center is taken to be the effective center of the source. The data are plotted in Figure 10 using the forward edge of the core as the effective center ([r - 0.3] m). For the 15-cm-Pb configuration, the graph is nearly flat, indicating consistency with an effective center at (r - 0.3) m. However, the data from the bare room do not show an obvious trend. At least one measurement may be inaccurate, or there may be some effects from the room-return neutrons that have not been characterized. The meaning of the data is not clear, and more measurements (with fission chambers and activation foils) may aid in the interpretation.

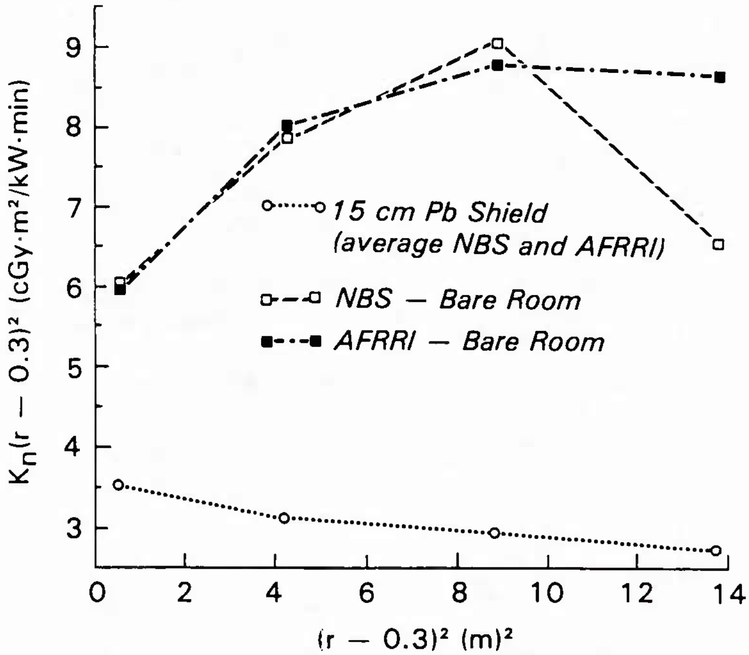

Figure 10. Neutron $1/(r-0.3)^2$ measurements (with 15 cm Pb or bare room)

POLARITY EFFECTS IN ER1

Appendix D provides the polarity data of the TE and Mg chambers from the measurements in ER1. In Appendix D, the ratio of +R to -R (+/-) is plotted for the TE and Mg chambers in the first and second sets of measurements. Differences of up to 30% in the chamber responses at opposite polarities were observed during the first set of measurements. Such large polarity effects are an indication of the presence of large spurious ionization currents from the cables and connectors. Before the second set of measurements, an attempt was made to reduce the polarity effect. The room was recabled, eliminating the patch panel inside the exposure room by running the signal cables straight to the readout room. In addition, lead bricks were used to shield the signal cables and the necessary connectors to the ionization chambers, but it was impractical to shield the cables immediately adjacent to the chambers. Although some improvement was seen in the AFRRI chambers, the recabling did not improve the large polarity differences of the NBS chambers. In fact, the NBS-observed polarity effects were even larger, and the effect was in the opposite direction for both groups. In spite of these large and inconsistent polarity effects, the average responses (average of +R and -R) of the AFRRI and NBS groups were in excellent agreement, indicating that averaging of the + and - chamber responses produces a reliable result.

However, the polarity problem should be considered when using small chambers to monitor experimental exposures. Generally, the polarity of the monitor chamber is not reversed, and therefore should be evaluated before each set of irradiations. If

significant changes are seen in the cable currents, then a correction should be applied. In any event, more work needs to be done to understand the cable-current problem and to reduce these sometimes anomalous effects.

DRIFT MEASUREMENTS

As discussed in the section on Chamber Response, the net chamber reading was determined by subtracting the average of the pre- and postirradiation drift readings from the chamber readings during irradiation. In the californium-252 facility, the drift readings were a measure of the system noise, but in the reactor facility the drift was actually a measure of the residual radiation in the exposure room. Although a portion of the residual radiation was a component of the measured gamma-ray kerma, it was subtracted to maintain consistency from day to day. This was necessary because the residual gamma radiation is, in some cases, very dependent on the core history.

The drift data for the AFRRI reactor exposures are summarized in Appendix E, where the drift data are plotted. These data indicate that with the lead shield in place, the residual radiation was a small percentage (~3%) of the total chamber reading, and the drift was not very dependent on core history. However, when the lead shield was moved away, the background radiation from the core constituted a much larger percentage of the total chamber reading (as high as 40%). Not only was the drift large in the unshielded configurations, but also it was very dependent on the core history. For example, the drift was lower at the beginning of the day and increased as the reactor core became more activated. In addition, the drift of the monitor chamber changed drastically in the unshielded configurations as the power increased from the very low levels (<0.1 kW) to the more routine power levels (>1 kW). One encouraging aspect of the unshielded data was that the monitor chamber and the measurement chambers (TE and Mg) showed similar patterns. That is, the changes in magnitude of the drift were about the same for the measurement and monitor chambers.

The drift data are tabulated in Appendix E, and the ratio of the postirradiation drift to preirradiation drift is shown for each chamber. For the lead-shielded configurations, the postirradiation drift was several times higher than the preirradiation drift (post/pre ranged from about 3 to 16), whereas this ratio was closer to 1 (1.1 to 4) for the unshielded radiations. Also, for all configurations, the ratio of post- to preirradiation drift increased as the chambers were moved farther from the core. This indicates that, closer to the core and without the lead shield, most of the drift results from the residual radiation of the core, whereas farther from the core or with the shield in place, the background radiation is mainly due to activation of products in the room (e.g., the lead shield, walls, and floor).

Although these observations are intuitive, they are important to remember when planning dosimetry for radiobiology experiments. Monitor chambers should be placed close to the subject of irradiation and should be filled with TE gas. This is to ensure that if the residual radiation changes significantly, the monitor chamber will in effect monitor the tissue kerma close to the experimental array. If several different dose rates (power levels) are to be used, the response of the monitor

compared to the dosimetry chambers should be evaluated at the different power levels. In addition, the residual radiation and its behavior with core history should be monitored closely for experiments in which the ratio K_g/K_T is crucial.

CONCLUSIONS

An extensive ionization-chamber intercomparison between NBS and AFRRI was completed using five radiation fields. The agreement between the two groups was good in the NBS californium-252 fields and excellent in the AFRRI reactor fields. Through the course of the study, the calibration procedures of AFRRI were validated, and many valuable data were collected concerning chamber characteristics and the spatial variation of tissue-kerma rates in two configurations of ER1.

In addition to these favorable results, the exercise itself proved to be an excellent opportunity for the AFRRI dosimetry program. Foremost was the valuable training experience afforded the AFRRI staff through the interaction with recognized experts in the radiation dosimetry field. Also, a guide to good dosimetry practices was prepared for AFRRI (19) as a direct result of the intercomparison. Finally, this work has resulted in the development of a long-term working relationship between the two groups, in which NBS will provide technical support to AFRRI in solving specific problems, and will assist AFRRI in maintaining continuity and reliability in its reactor dosimetry program.

APPENDIX A. RADIATION SCHEDULE

Date	Source
5-8 July 1983	NBS californium-252 source
18-22 July 1983	AFRRI TRIGA reactor
7 November 1983	NBS cobalt-60 source
8-11 November 1983	NBS californium-252 source
27 February- 7 March 1984	AFRRI TRIGA reactor

APPENDIX B. CALCULATION OF k_t

$$k_t = \frac{W_c}{W_n} \frac{(s_{m,g})_c}{(r_{m,g})_n} \frac{[(\mu_{en}/\rho)_t / (\mu_{en}/\rho)_m]_c}{(K_t/K_m)_n}$$

where c = calibration gamma rays (cobalt-60)

n = neutrons in the mixed field

W = average energy required to produce an ion pair in the cavity gas (Table 2)

$s_{m,g}$ = wall-to-gas restricted collision mass-stopping power ratio of 1

$r_{m,g}$ = gas-to-wall absorbed-dose conversion factor for the non-Bragg-Gray cavity conditions generally produced by neutrons of 0.99

$(K_t/K_m)_n$ = ratio of neutron kerma in tissue to the neutron kerma in the chamber materials

APPENDIX C. MONITOR CHAMBER RESPONSE

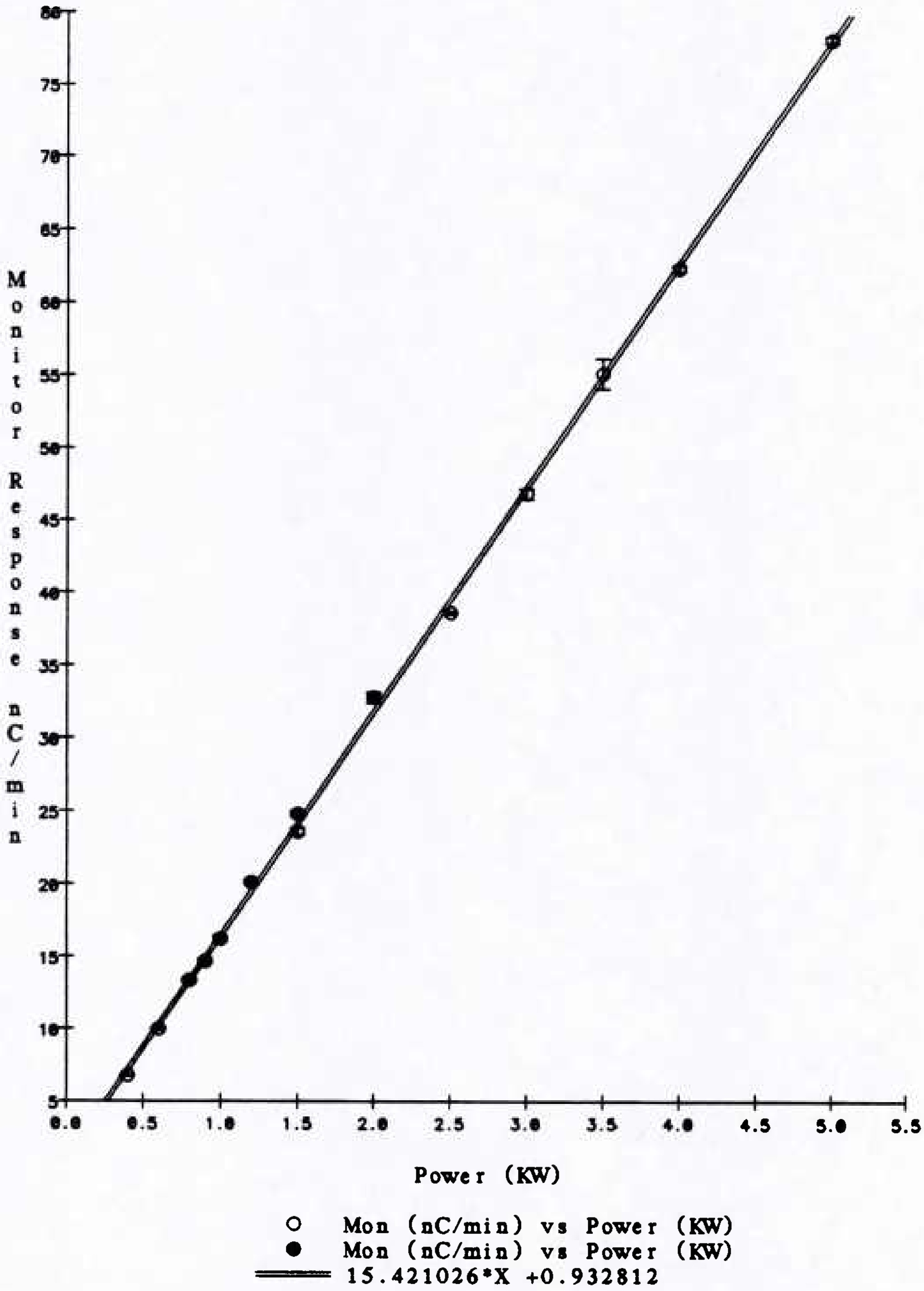

Figure 11. Monitor response in ER1 with 15-cm-Pb shield

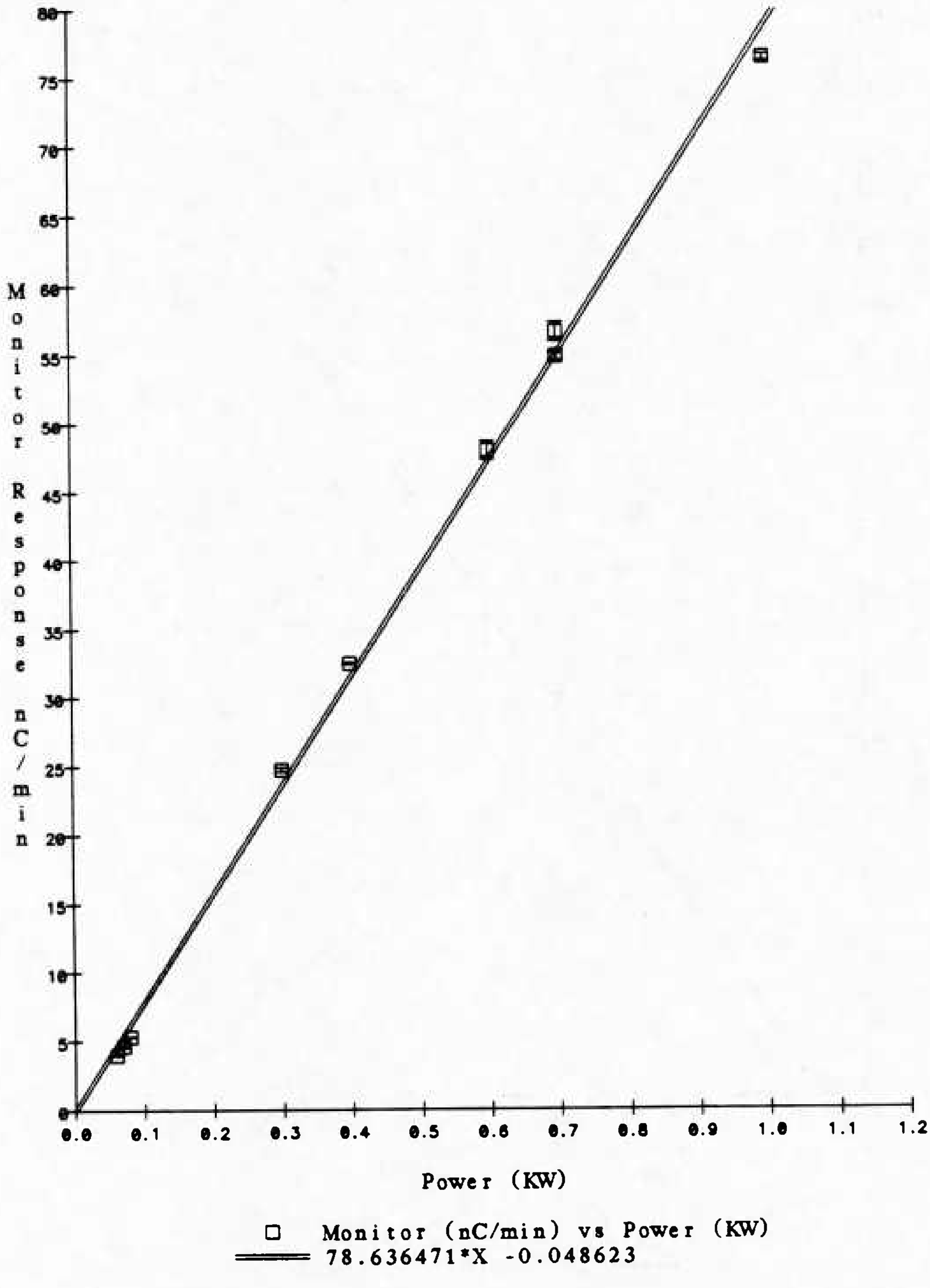

Figure 12. Monitor response in ER1 with no shield (bare room)

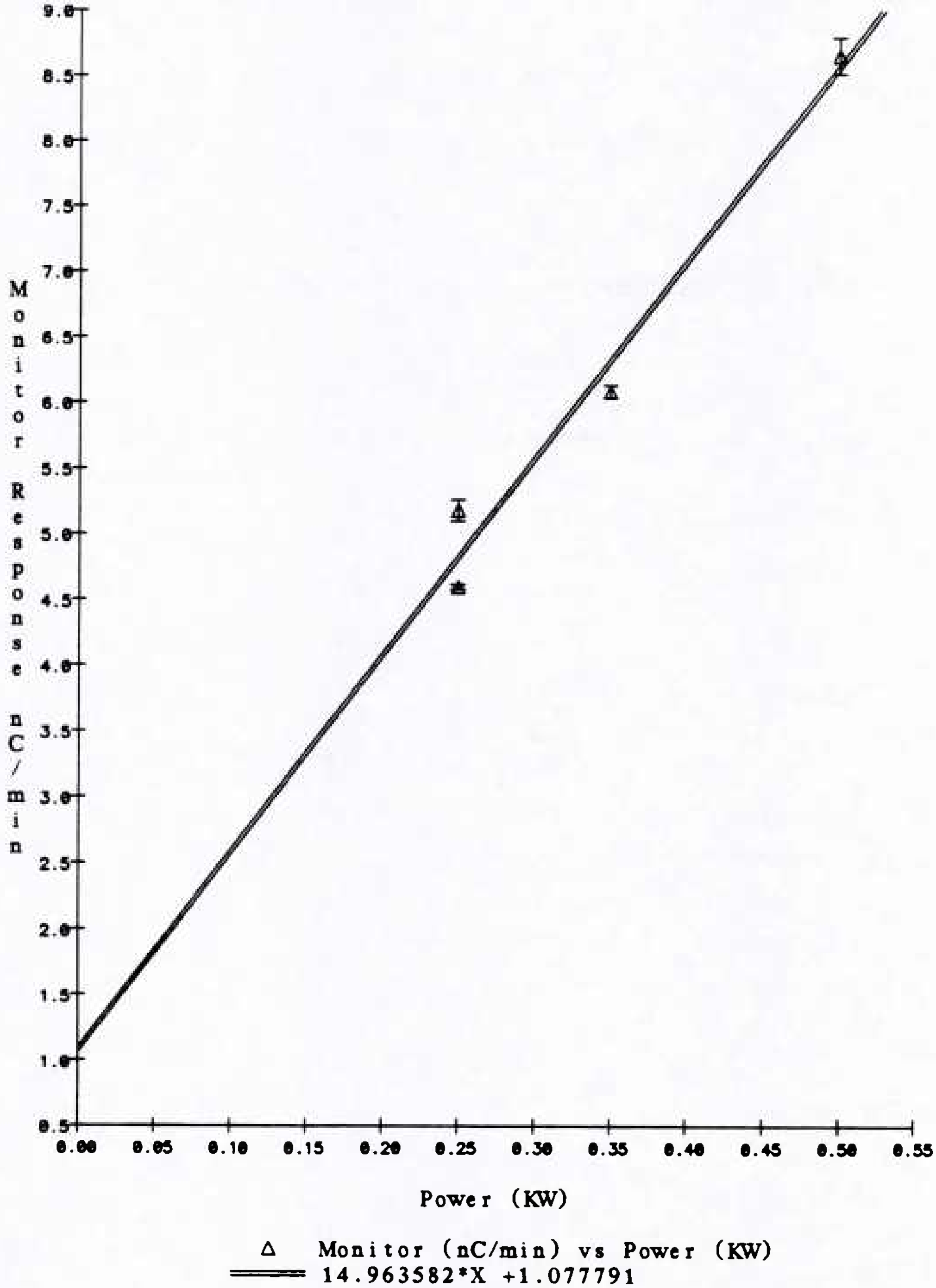

Figure 13. Monitor response in ER1 with 30-cm-water shield

Table 7. Conversion From Monitor Readings to cGy/kW · min

Configuration	Distance of Dosimetry Chambers From Tank Wall (cm)	Power (kW)	cGy/kW · min per µGy/pCm
15 cm Pb	70	0.4	1.775
	205	2.5	1.579
	298	3.5	1.568
	371	4.0	1.565
In phantom	70	1.0	1.636
Bare room	70	0.075	7.799
	205	0.350	7.850
	298	0.650	7.856
	371	0.850	7.856
30 cm water	70	0.500	1.730

APPENDIX D. POLARITY EFFECTS DATA

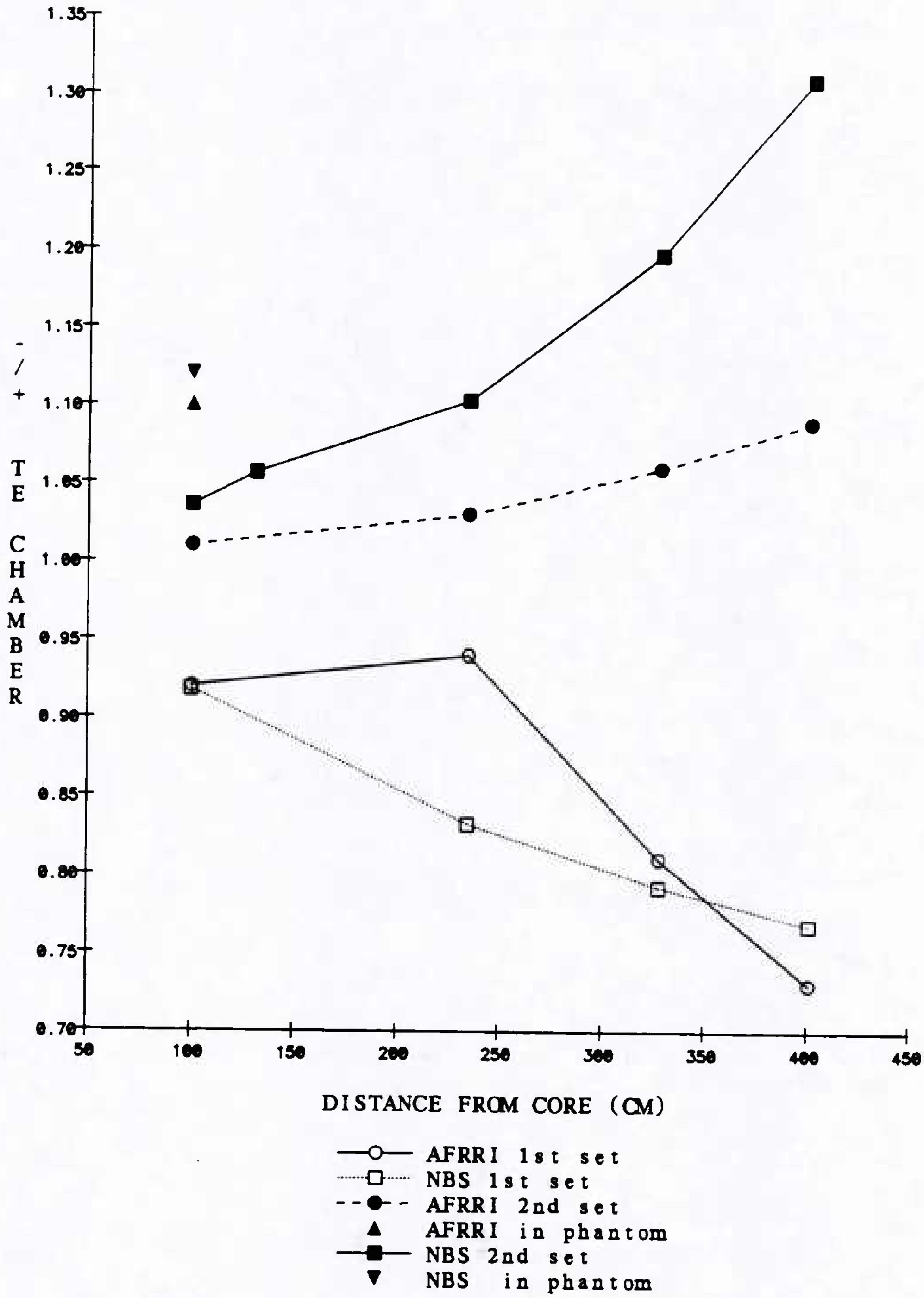

Figure 14. TE chamber polarity effects with 15-cm-Pb shield

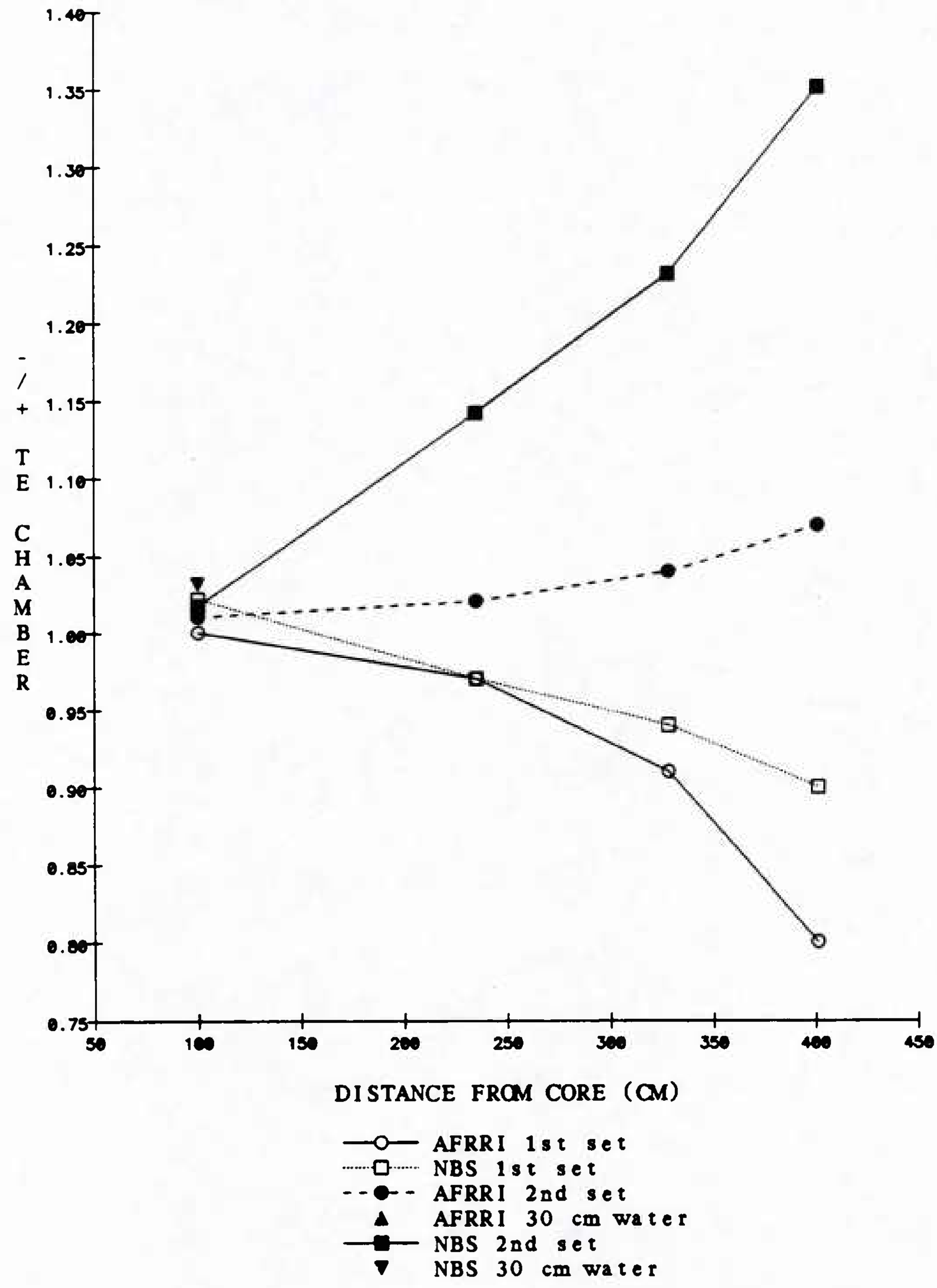

Figure 15. TE chamber polarity effects in bare room and with 30-cm-water shield

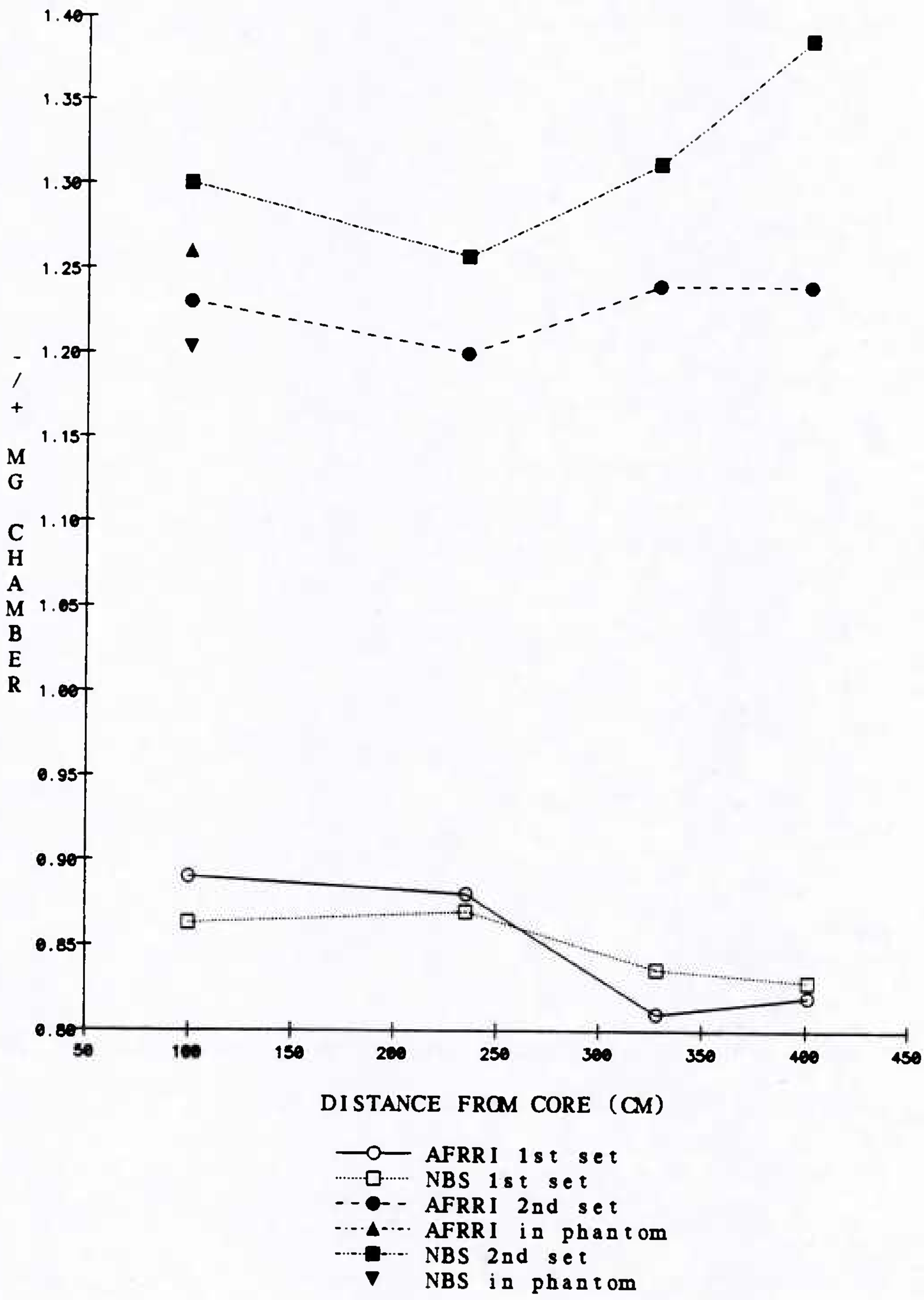

Figure 16. MG chamber polarity effects with 15-cm-Pb shield

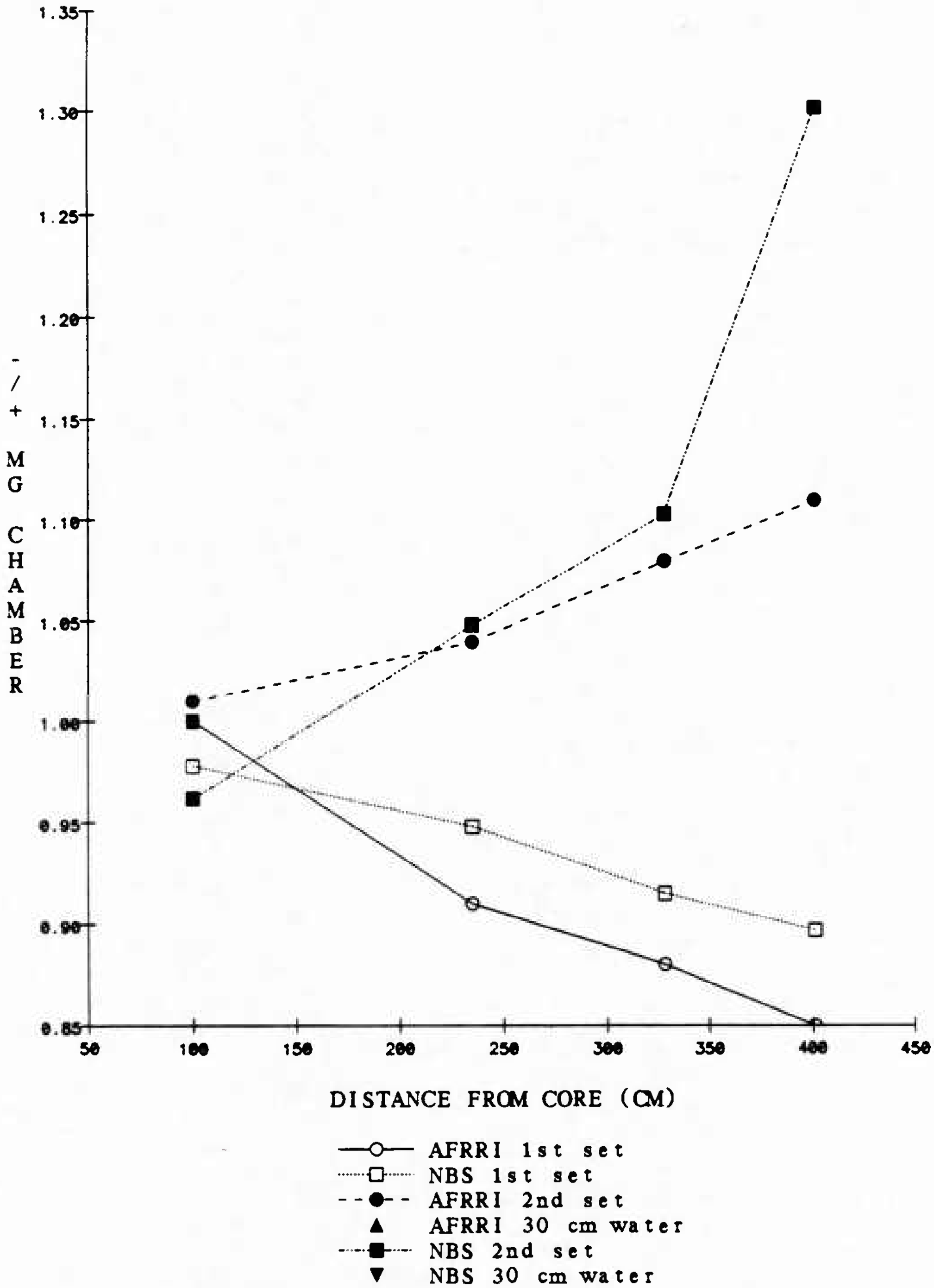

Figure 17. MG chamber polarity effects in bare room and with 30-cm-water shield

APPENDIX E. DRIFT DATA

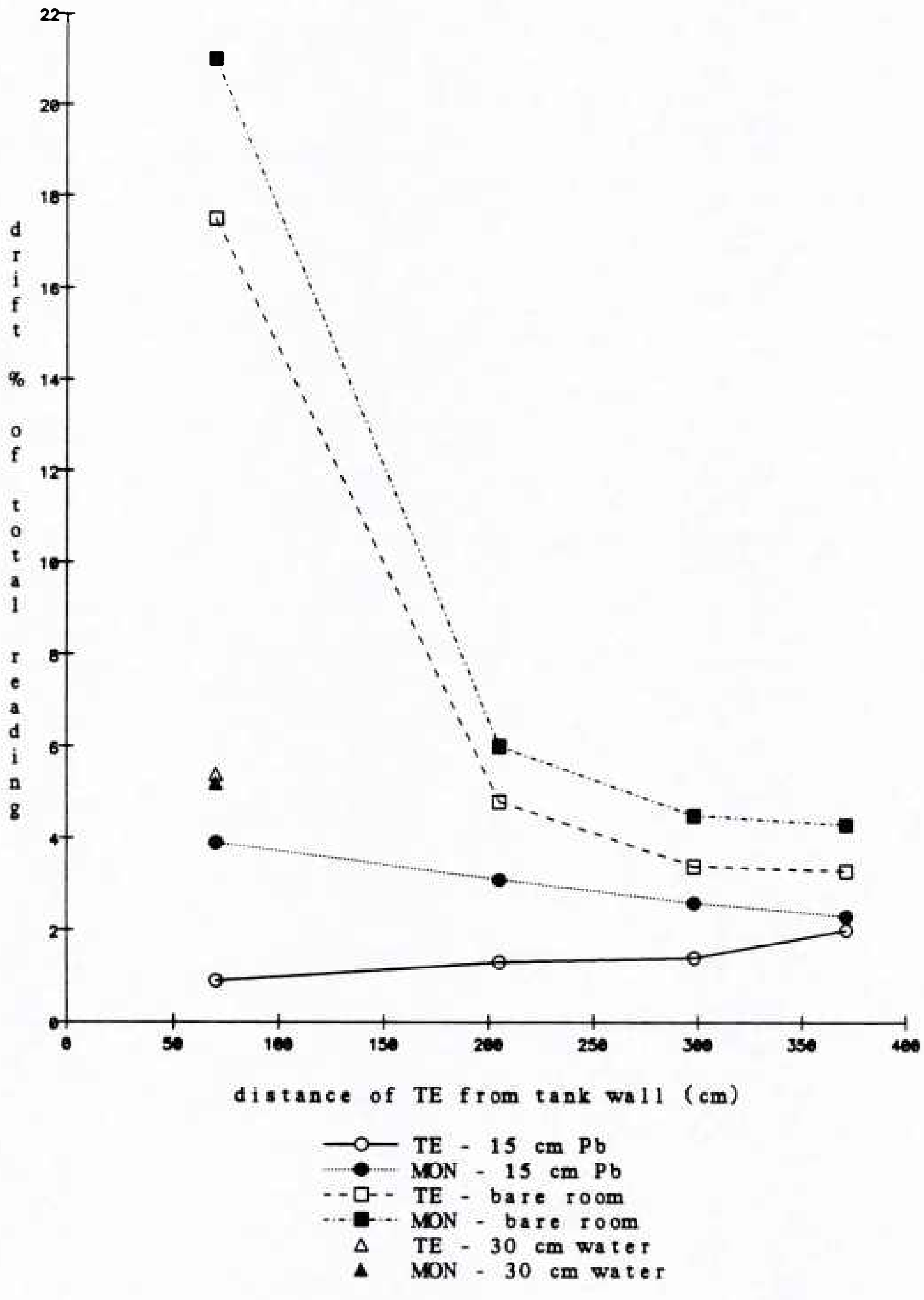

Figure 18. TE and monitor chambers drift data

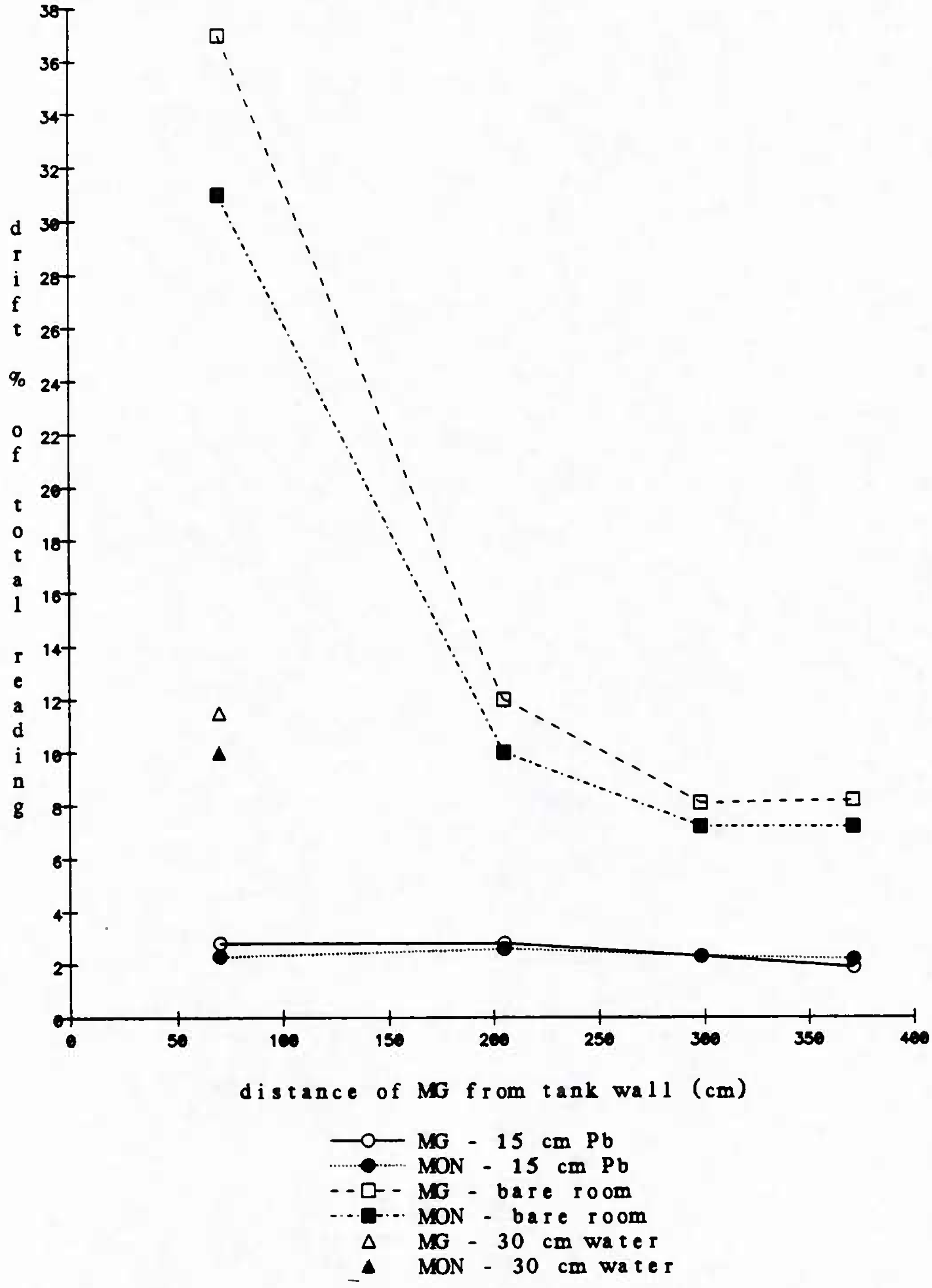

Figure 19. Mg and monitor chambers drift data

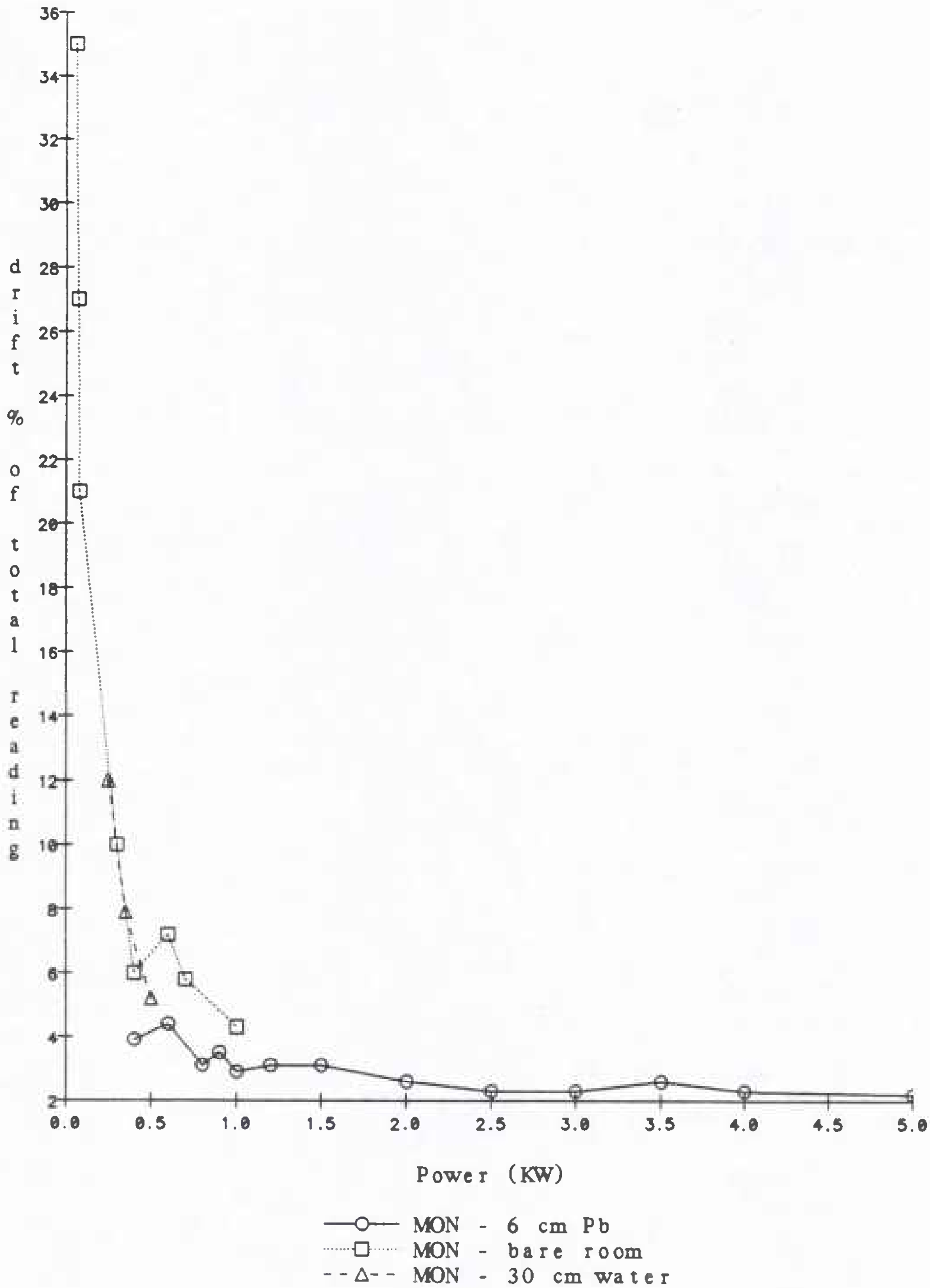

Figure 20. Monitor chamber drift versus reactor power

Table 8. Chamber Drift Data

Configuration	Distance From Tank Wall (cm)	Power (kW)	Drift (% of Total Reading)			Post/Pre*		
			TE	Mg	Monitor	TE	Mg	Monitor
15 cm Pb	70	0.4	0.9		3.9	5.0		2.8
	101	0.6	1.1		3.9	3.9		2.8
	205	1.5	1.3		3.1	4.1		4.0
	298	2.0	1.4		2.6	3.0		7.5
	371	3.0	2.0		2.3	2.3		9.3
In phantom	70	0.9	1.0		3.5	3.5		4.5
15 cm Pb	70	2.5		2.8	2.2		5.7	7.7
	205	3.5		2.8	2.6		11.0	9.7
	298	4.0		2.3	2.3		16.0	8.0
	371	5.0		1.9	2.2		7.4	10.0
In phantom	70	1.5		1.9	3.5		6.9	4.5
Bare room	70	0.08	18.0		21.0	1.2		1.2
	205	0.40	4.8		6.0	2.6		2.3
	298	0.70	3.4		4.5	3.4		3.0
	371	1.00	3.3		4.3	4.0		3.7
30 cm water	70	5.00	5.4		5.2	2.8		2.7
Bare room	70	0.06		41.0	35.0		1.1	1.1
	70	0.07		33.0	27.0		1.1	1.1
	205	0.30		12.0	10.0		1.6	1.7
	298	0.60		8.1	7.2		1.9	2.1
	371	0.70		8.2	7.2		1.8	2.1
30 cm water	70	0.25		14.0	12.0		1.5	1.5
	70	0.35		9.0	7.9		2.1	1.9

*Ratio of postirradiation drift to preirradiation drift

REFERENCES

1. An international neutron dosimetry intercomparison. ICRU Report 27. International Commission on Radiation Units and Measurements, Washington, DC, 1978.

2. Average energy required to produce an ion pair. ICRU Report 31. International Commission on Radiation Units and Measurements, Washington, DC, 1979.

3. Waterman, F. M., Kuchnir, F. T., Skaggs, L. S, Kouzes, R. T., and Moore, W. H. Energy dependence of the neutron sensitivity of C-CO_2, Mg-Ar, and TE-TE ionization chambers. Physical Medical Biology 24: 721-733, 1979.

4. Goodman, L. J., and Coyne, J. J. W_n and neutron kerma for methane-based tissue-equivalent gas. Radiation Research 82: 13-26, 1980.

5. Mijnheer, B. J. The relative neutron sensitivity, k_u, for non-hydrogenous detectors. In: Ion Chambers for Neutron Dosimetry. CEC Report EUR 6782 EN. Broerse, J. J., ed. Harwood Academic Publishers, New York, 1980.

6. Caswell, R. S., Coyne, J. J., and Randolph, M. L. Kerma factors of elements and compounds for neutron energies below 30 MeV. International Journal of Applied Radiation Isotopes 33: 1227-1262, 1982.

7. Verbinski, V. V., Cassapakis, C. C., Hagan, W. K., Ferlic, K., and Daxon, E. Radiation field characterization for the AFRRI TRIGA reactor. Vol. I: Baseline data and evaluation of calculational data. DNA Report No. 5793F-1. Defense Nuclear Agency, Washington, DC, 1981.

8. Verbinski, V. V., Cassapakis, C. C., Hagan, W. K., Ferlic, K., and Daxon, E. Calculation of the neutron and gamma-ray environment in and around the AFRRI TRIGA reactor, Vol. II. DNA Report No. 5793F-2. Defense Nuclear Agency, Washington, DC, 1981.

9. Ferlic, K. P., and Zeman, G. H. Spectrum-averaged kerma factors for reactor dosimetry with paired ion chambers. Technical Report TR83-2. Armed Forces Radiobiology Research Institute, Bethesda, Maryland, 1983.

10. Neutron dosimetry for biology and medicine. ICRU Report 26. International Commission on Radiation Units and Measurements, Washington, DC, 1977.

11. Protocol for neutron beam dosimetry. AAPM Report No. 7 of Task Group 18, Fast Neutron Beam Physics. Radiation Therapy Committee, American Association of Physicists in Medicine, 1980.

12. Broerse, J. J., Mijnheer, B. J., and Williams, J. R. European protocol for neutron dosimetry for external beam therapy. British Journal of Radiology 54: 882-898, 1981.

13. Grundl, J. A., and Eisenhauer, C. M. Fission spectrum neutrons for cross section validation and neutron flux transfer. Proceedings of Conference on Nuclear Cross Sections and Technology, NBS Special Publication 425, US Department of Commerce, Washington, DC, March, 1975.

14. Grundl, J. A., and Eisenhauer, C. M. Compendium of benchmark neutron fields for reactor dosimetry, standard neutron field entries. NBS IR 85-3151, US Department of Commerce, Washington, DC, January, 1986.

15. Sholtis, J. A., Jr., and Moore, M. L. Reactor facility at Armed Forces Radiobiology Research Institute. Technical Report TR81-2. Armed Forces Radiobiology Research Institute, Bethesda, Maryland, 1981.

16. Sayeg, J. A. Neutron and gamma dosimetry measurements at the AFRRI-DASA TRIGA reactor. Contract Report CR65-6. Armed Forces Radiobiology Research Institute, Bethesda, Maryland, 1965.

17. Zeman, G. H., and Dooley, M. A. Performance and dosimetry of Theratron-80 cobalt-60 unit at Armed Forces Radiobiology Research Institute. Technical Report TR84-1. Armed Forces Radiobiology Research Institute, Bethesda, Maryland, 1984.

18. Wycoff, H. O. Reply to corrected f factors for photons from 10 KeV to 2 MeV. Medical Physics 10: 715-716, 1983.

19. Goodman, L. J. A practical guide to ionization chamber dosimetry at the AFRRI reactor. Contract Report CR85-1. Armed Forces Radiobiology Research Institute, Bethesda, Maryland, 1985.

20. Boag, J. W. Ionization chambers. In: Radiation Dosimetry, Vol. II. Attix, R. H., Roesch, W. C., and Tochilin, E., eds. Academic Press, New York, 1966, pp. 11-41.

21. Goodman, L. J., Coyne, J. J., Zoetelief, J., Broerse, J. J., and McDonald, J. C. Dosimetry of a lightly encapsulated Cf-252 source. Radiation Protection Dosimetry 4(2): 91-96, 1983.